Biogeosciences Discuss., doi:10.5194/bg-2016-441, 2016
Manuscript under review for journal Biogeosciences
Published: 21 October 2016

Biogeosciences Discussions
Open Access
EGU

Evaluating the Community Land Model (CLM 4.5) at a Coniferous Forest Site in Northwestern United States Using Flux and Carbon-Isotope Measurements

Henrique F. Duarte[1], Brett M. Raczka[2], Daniel M. Ricciuto[3], John C. Lin[1], Charles D. Koven[4], Peter E. Thornton[3], David R. Bowling[2], Chun-Ta Lai[5], Kenneth J. Bible[6], James R. Ehleringer[2]

[1]Department of Atmospheric Sciences, University of Utah, Salt Lake City, 84112, USA
[2]Department of Biology, University of Utah, Salt Lake City, 84112, USA
[3]Oak Ridge National Laboratory, Oak Ridge, 37831, USA
[4]Lawrence Berkeley National Laboratory, Berkeley, 94720, USA
[5]Department of Biology, San Diego State University, San Diego, 92182, USA
[6]United States Forest Service, Pacific Northwest Research Station, Corvallis, 97331, USA

Correspondence to: Henrique F. Duarte (h.duarte@utah.edu)

Abstract. Summer droughts in the western United States are expected to intensify with climate change. Thus, an adequate representation of ecosystem drought response in land models is critical for predicting carbon dynamics. The goal of this study was to assess the performance of the Community Land Model, Version 4.5 (CLM) for an old-growth coniferous forest in the Pacific Northwest region of the United States (Wind River AmeriFlux site), characterized by a climate that has heavy winter precipitation followed by summer drought. Particular attention was given to the model skill in the simulation of stomatal conductance and its response to drought stress. CLM was driven by site-observed meteorology and calibrated primarily using parameter values observed at the site or at similar stands in the region. Key model adjustments included parameters controlling specific leaf area and stomatal conductance. Default values of these parameters led to significant underestimation of gross primary production, overestimation of evapotranspiration, and consequently overestimation of photosynthetic ^{13}C discrimination, reflected on reduced ^{13}C:^{12}C ratios of carbon fluxes and pools. Adjustments in soil hydraulic parameters within CLM were also critical, preventing significant underestimation of soil water content and unrealistic drought stress during summer. After calibration, CLM was able to simulate energy and carbon fluxes, leaf area index, biomass stocks, and carbon isotope ratios of carbon fluxes and pools in reasonable agreement with site observations. Overall, the calibrated CLM was able to simulate the observed response of canopy conductance to atmospheric vapor pressure deficit and soil water content, reasonably capturing the impact of drought stress on ecosystem functioning. The calibrated parameters may be of use for future modeling studies involving stands of similar age and composition under a similar climate regime. More broadly, the calibration of the Ball-Berry stomatal conductance model in CLM aligned with observations reported in the literature for coniferous trees, suggesting that a future release of CLM would benefit from using a distinct, lower slope value ($m_{bb} = 6$) for conifers, rather than a unique value for all C3 plants ($m_{bb} = 9$). Thanks to the recent implementation of photosynthetic ^{13}C discrimination within CLM, the results of this study indicate that carbon isotope

Biogeosciences Discuss., doi:10.5194/bg-2016-441, 2016
Manuscript under review for journal Biogeosciences
Published: 21 October 2016

measurements can be used to constrain stomatal conductance and water use efficiency in CLM as an alternative to flux observations. They also have the potential to guide structural improvements in the model in respect to the representation of carbon storage pools.

1 Introduction

The frequency, duration, and severity of droughts are expected to increase in the 21st century with climate change (Burke et al., 2006; Sheffield and Wood, 2008; Dai, 2013; Prein et al., 2016). In the western United States in particular, the combination of warmer temperature, larger vapor pressure deficit, reduced snowfall and snow pack, earlier snow melt, and extended growing season length is expected to lead to an intensification of summer droughts (Boisvenue and Running, 2010; Spies et al., 2010; Swain and Hayhoe, 2015). In this drying scenario, an accurate representation of ecosystem drought response in land models is critical for projecting carbon dynamics (and climate) into the future.

Leaf gas exchange, including CO_2 uptake from photosynthesis and water vapor loss via transpiration, is controlled by leaf stomata. Stomatal conductance responds to drought and various other environmental factors, but its modeling still represents a major challenge for the scientific community (Damour et al., 2010). Many stomatal conductance models have been proposed, including different approaches to account for drought stress, but each model has its own limitations (see the detailed review by Damour et al., 2010).

During photosynthesis, plants discriminate against the heavier stable isotope of carbon (^{13}C) in favor of the lighter, more abundant ^{12}C stable isotope. This discrimination in C3 plants, expressed as $\Delta = \left[\left(R_{air}/R_{plant}\right) - 1\right] \times 1000$ (‰), where R_{air} and R_{plant} are the ^{13}C:^{12}C isotope ratios of atmospheric CO_2 and plant assimilated carbon, respectively, can be estimated according to the model proposed by Farquhar and Richards (1984) as

$$\Delta = a + (b - a)c_i/c_a \,, \quad (1)$$

where c_i/c_a is the ratio of intercellular CO_2 concentration to atmospheric CO_2 concentration, a is the ^{13}C discrimination associated with the process of CO_2 diffusion through the stomata, and b is the ^{13}C discrimination associated with the process of assimilation of CO_2 via Rubisco ($a \approx 4.4$‰ and $b \approx 27$‰; Farquhar et al., 1989). The c_i/c_a ratio correlates negatively with leaf intrinsic water use efficiency, defined as the ratio of net leaf assimilation to stomatal conductance (Farquhar et al., 1989). Under drought stress, C3 plants tend to reduce stomatal conductance and increase water use efficiency, leading to reductions in c_i/c_a and ^{13}C discrimination, affecting the carbon isotope ratio ($\delta^{13}C$) of photosynthate and consequently of carbon pools and fluxes. Experimental studies have shown, for instance, correlations between the $\delta^{13}C$ of ecosystem respiration and soil water content, atmospheric vapor pressure deficit, and precipitation (see Bowling et al., 2008 and Brüggemann et al., 2011 for extensive reviews of experimental results on the link between environmental factors and the isotopic signature of carbon pools and fluxes). Isotopic measurements can therefore be used to gain insights about the response of stomatal conductance and water use efficiency to drought.

Biogeosciences Discuss., doi:10.5194/bg-2016-441, 2016
Manuscript under review for journal Biogeosciences
Published: 21 October 2016

Photosynthetic ^{13}C discrimination has been included in the latest release of the Community Land Model (CLM v.4.5, hereafter referred to as CLM). CLM is the land model component of the Community Earth System Model (CESM), a fully-coupled, global climate model widely used by the scientific community. Revised photosynthesis and hydrology schemes, among an extensive list of updates have also been included in CLM (Oleson et al., 2013).

The goal of the present study is to evaluate the performance of CLM for a coniferous forest site in the Pacific Northwest region of the United States (Wind River AmeriFlux site), with particular attention to the simulation of stomatal conductance and its response to changes in atmospheric vapor pressure deficit and soil water content associated with summer drought. For this evaluation, this study uses not only observed surface fluxes, leaf area index, and biomass stocks as reference values, but also observed $\delta^{13}C$ values of carbon fluxes and pools, taking advantage of the recent inclusion of photosynthetic ^{13}C discrimination within the model.

2 Material and Methods

This Section provides a description of CLM, focusing on key formulations of relevance to the present study (Sect. 2.1), followed by a description of the study site (Sect. 2.2), the eddy-covariance and meteorological data sets used to drive and assess the model (Sect. 2.3), the carbon isotope data sets used to assess the photosynthetic ^{13}C discrimination in CLM (Sect. 2.4), and also a description of the CLM configuration, simulations performed, and calibration of model parameters (Sects. 2.5 and 2.6). Section 2.7 describes the methodology used in the calculation of canopy conductance values from eddy-covariance observations, which are compared against simulated values as a way to assess the model skill in simulating leaf stomatal conductance.

2.1 Model Description

This Section focuses on describing CLM's approach to the simulation of stomatal conductance and photosynthetic ^{13}C discrimination, key aspects of this study. For a full description of the model, the reader is referred to Oleson et al. (2013).

In CLM, leaf stomatal conductance (g_s) is calculated based on the Ball-Berry model as described by Collatz et al. (1991) and implemented by Sellers et al. (1996) in the SiB2 model:

$$g_s = m_{bb} \frac{A_n(\beta_t)}{c_s/P_{atm}} h_s + b_{bb}\beta_t \quad (2)$$

where $A_n(\beta_t)$ is the net leaf photosynthesis as a function of a drought stress factor (β_t), c_s is the CO_2 partial pressure at the leaf surface, P_{atm} is the atmospheric pressure, h_s is the relative humidity at the leaf surface (defined as the ratio of vapor pressure at the leaf surface to saturation vapor pressure inside the leaf at vegetation temperature T_v), m_{bb} is a slope coefficient, and b_{bb} corresponds to the minimum stomatal conductance in the original Ball-Berry model. The drought stress factor β_t is defined as:

$$\beta_t = \sum_i w_i r_i \quad (3)$$

Biogeosciences Discuss., doi:10.5194/bg-2016-441, 2016
Manuscript under review for journal Biogeosciences
Published: 21 October 2016

where r_i is the root fraction at soil layer i and w_i is a corresponding plant wilting factor, calculated as a function of soil water potential and a plant-dependent response to drought stress. The sum in Eq. (3) is defined over the entire soil column, resulting in β_t values from 0 (maximum drought stress) to 1 (no drought stress). In CLM's implementation of the Ball-Berry model (Eq. 2), β_t is used to downscale b_{bb}, directly impacting g_s. β_t also indirectly impacts g_s through the A_n term, as β_t is used to downscale the maximum rate of carboxylation ($\beta_t V_{cmax}$) and also leaf respiration ($\beta_t R_d$) (Oleson et al., 2013).

The implementation of photosynthetic ^{13}C discrimination in CLM for C3 plants follows the model proposed by Farquhar and Richards (1984) (cf. Eq. 1):

$$\Delta = 4.4 + 22.6\, c_i/c_a. \tag{4}$$

CLM calculates the intercellular-to-atmospheric CO_2 concentration ratio, c_i/c_a, as:

$$\frac{c_i}{c_a} = 1 - \frac{A_n(1-d)}{c_a}\left[\frac{1.4}{g_b} + \frac{1.6}{g_s}\right] \tag{5}$$

where d is a downregulation factor associated with nitrogen limitation and g_b is the leaf boundary layer conductance. Assuming $g_b \gg g_s$ (typically true for coniferous needles), Eq. (5) can be approximated by:

$$\begin{aligned}\frac{c_i}{c_a} &\cong 1 - \frac{1.6(1-d)}{c_a}\left[\frac{A_n}{g_s}\right] \\ &\cong 1 - \frac{1.6(1-d)}{c_a}\,\mathrm{iWUE}\end{aligned} \tag{6}$$

where $\mathrm{iWUE} = A_n/g_s$ is the intrinsic water use efficiency. Note that c_i/c_a and consequently Δ correlate negatively with iWUE. All other terms being constant in Eq. (6), an increase in iWUE is expected to result in a reduction of the photosynthetic ^{13}C discrimination, i.e., an increase in the assimilation of the heavier ^{13}C stable isotope relative to the lighter, more abundant ^{12}C stable isotope.

2.2 Site Description

The chosen site for this study–Wind River–is part of the AmeriFlux eddy covariance network (Baldocchi et al., 2001) with a long record of meteorological, biological, surface flux (energy and carbon), and carbon isotope measurements for model assessment (1998–present). The site is located in the Pacific Northwest region of the United States, in the state of Washington (45.8205 Lat, −121.9519 Lon, 371-m elevation — see Fig. 1). Wind River is characterized by an old-growth conifer forest dominated by Douglas-fir (*Pseudotsuga menziesii*) and western hemlock (*Tsuga heterophylla*) trees, with a mean canopy height of 56 m. Douglas-fir trees are about 40–65-m high, corresponding to about 50% of the wood volume of the stand and 33% of the leaf area, while western hemlock trees are more numerous and smaller, corresponding to about 53% of the leaf area of the stand (Unsworth et al., 2004; Parker et al., 2004). No significant disturbances have occurred at the site in the past ~450–500 years. The local climate is strongly seasonal, marked by annual summer drought and wet winters. The climate summary reported by Shaw et al. (2004) indicates a mean annual precipitation of 2223 mm, with only ≈5% falling during June, July, and August. During winter, much of the precipitation falls as snow, and the average snowpack depth

Biogeosciences Discuss., doi:10.5194/bg-2016-441, 2016
Manuscript under review for journal Biogeosciences
Published: 21 October 2016

exceeds 100 mm. The mean annual, January, and July air temperatures are 8.7±6.5 °C, 0.1±2.3 °C, and 17.7±1.7 °C, respectively.

2.3 Eddy-Covariance and Meteorological Data

Air temperature, relative humidity, wind speed, incident short-wave radiation, incident long-wave radiation, atmospheric pressure, and precipitation observed at the Wind River site from 1998 to 2006 were used to drive CLM. The time series were gap-filled using data from nearby towers and climate stations or interpolated in case of missing data. The gap-filled data product used to drive CLM in this study was created at Oak Ridge National Laboratory following the methodology described in Barr et al. (2013).

The L4 data set based on the eddy-covariance observations was downloaded from the AmeriFlux repository (version V002, daily averages). This data set contains friction-velocity-filtered, gap-filled, and partitioned fluxes and was used to assess the simulated surface fluxes of sensible heat (H), latent heat (LE), and carbon, including gross primary production (GPP) and ecosystem respiration (ER). The ER product was estimated according to the short-term temperature response of measured nighttime net ecosystem exchange (NEE) (Reichstein et al., 2005), and GPP as the difference between ER and NEE: i.e., $\mathrm{ER} - \mathrm{NEE}$. The gap-filled NEE values (and derived GPP and ER) using the Marginal Distribution Sampling method (Reichstein et al., 2005) were used in this study.

Eddy-covariance and meteorological data from the AmeriFlux L2 data product (version V007, 30-min averages) were used to calculate canopy conductance (G_c, see Sect. 2.7) and atmospheric vapor pressure deficit (VPD). L2 soil water content (SWC) data were also used in the analysis. Missing SWC data from the L2 dataset in the year 2002 were replaced by respective L1 data (version Apr2013). In the analysis, 30-min surface flux data were rejected during periods when the wind direction was in the $[45^{o} : 135^{o}]$ sector (same criterion used by Wharton et al., 2012), as the northeast-to-southeast wind sector is characterized by heterogeneous (age-fragmented) land cover. The data were hourly averaged prior to G_c and VPD calculation.

2.4 Carbon Isotope Data

Estimated $\delta^{13}C$ values of ER (Lai et al., 2005) and observed $\delta^{13}C$ values of leaf tissue and soil organic matter (Fessenden and Ehleringer, 2003) at Wind River were used to assess the photosynthetic ^{13}C discrimination in CLM.

Lai et al. (2005) used an automated air sampling system, with inlets at 0.5 m above ground level and at 0.5 canopy height, collecting 15 flasks weekly during the growing season. 13 of the 15 flasks were dedicated to nighttime sampling (over a single night). The Keeling-plot method was used to infer the weekly $\delta^{13}C_{ER}$ using the CO_2 and $\delta^{13}CO_2$ observations (for simplicity, the resulting $\delta^{13}C_{ER}$ values are referred to as "observations" in the text). The monthly averages (June–November) from 2001 to 2003 reported by Lai et al. (2005) were used as reference in the present study.

Fessenden and Ehleringer (2003) conducted measurements of $\delta^{13}C$ of bulk organic tissue from current-year needles of *Tsuga heterophylla* trees and seedlings at the top (55 m), middle (25 m), and bottom (2 m) of the canopy. They also

Biogeosciences Discuss., doi:10.5194/bg-2016-441, 2016
Manuscript under review for journal Biogeosciences
Published: 21 October 2016

conducted vertical profile measurements of $\delta^{13}C$ of bulk soil organic carbon down to 20-cm depth. The measurements were performed on a 1-month to 2-month time interval. The values reported by Fessenden and Ehleringer (2003) for the growing season in 1999 and 2000 were used as reference.

In the present study, both observed and modeled carbon isotope ratios were expressed as $\delta^{13}C = \left(\frac{R_x}{R_{std}} - 1\right) \times 1000$ (‰), where R_x is the ^{13}C:^{12}C isotope ratio of the carbon pool/flux of interest and R_{std} is the ^{13}C:^{12}C isotope ratio of a standard reference material (Vienna Pee Dee Belemnite standard).

2.5 CLM Configuration and Simulations

CLM was run at site level using the PTCLM scripting framework (see Kluzek, 2013), as in recent studies (e.g., Mao et al., 2016; Raczka et al., 2016). Land cover was defined as the needleleaf evergreen temperate tree plant functional type. The model was configured to use CLM v.4.5 physics and CLM v.4.5 CN biogeochemistry. The vertical soil carbon profile option was turned on, and the CENTURY Carbon model was selected for the decomposition parameters. The nitrification and de-nitrification sub-model was switched off, as preliminary simulations indicated an excess of nitrogen availability and forest productivity when the respective module was active. Given that the Wind River site is characterized by an old-growth mature forest, no land-cover disturbance was considered in the simulations.

The model was spun-up in a two-stage process, using a pre-industrial component set with a constant, pre-industrial atmospheric CO_2 concentration and $\delta^{13}CO_2$ of 285 ppmv and −6.5‰, respectively. The model was run in accelerated decomposition mode for 600 years (first stage) and then in normal decomposition mode for 1000 years (second and final stage), using the local observed meteorological data (Sect. 2.3) from 1998 to 2006 to drive the model (continuously cycled). Following the spin-up process, a transient run (1850–2006) was performed with prescribed nitrogen deposition, atmospheric CO_2 concentration, and atmospheric $\delta^{13}CO_2$.

The transient atmospheric CO_2 concentrations used in this study were based on the CMIP5 recommendations for annual global mean values (Meinshausen et al., 2011). The transient atmospheric $\delta^{13}CO_2$ values used here were based on ice-core and flask measurements reported by Francey et al. (1999) (annual values in their spline fitting from 1850 to 1981) and flask measurements in Mauna Loa (annual averages from 1981 to 2006) by the Scripps CO_2 program (Keeling et al., 2005), following a similar methodology as in Raczka et al. (2016). As in the spin-up process, the local observed meteorological data from 1998 to 2006 were cycled during the transient run. The driver-data and model years were aligned in a way to guarantee a perfect match between them during the final 9 years of the simulation (1998–2006).

2.6 CLM Calibration

Initial simulations using the default parameters from CLM resulted in a poor representation of the carbon dynamics at the Wind River site. GPP and forest biomass were significantly underestimated. The seasonality of ER was poorly represented and the simulated late-summer GPP was impacted by an underestimation of SWC, resulted from a poor

Biogeosciences Discuss., doi:10.5194/bg-2016-441, 2016
Manuscript under review for journal Biogeosciences
Published: 21 October 2016

representation of soil hydrology at the site. Furthermore, the modeled evapotranspiration values were significantly overestimated. As a result of CLM's poor performance in the simulation of GPP and evapotranspiration, the modeled photosynthetic ^{13}C discrimination was found to be overestimated, reflected on reduced ^{13}C:^{12}C ratios of carbon fluxes and pools.

In order to improve the representation of the carbon dynamics at the site, key model parameters were calibrated as detailed in Appendix A and summarized in Table 1. The adjusted parameters were primarily based on biological measurements at Wind River or at similar stands in the Pacific Northwest. Parameters controlling specific leaf area and stomatal conductance were found to be critical to the simulation of GPP and evapotranspiration and were adjusted in a way to minimize the differences between model output and site observations (eddy covariance fluxes). The default soil hydraulic parameters used in CLM version 4.5 were found to be inadequate at Wind River, leading to severe underestimation of SWC and unrealistic drought stress in the model during late summer. These parameters were reverted back to their default values in CLM version 4.0, with significant improvement in the representation of soil hydrology at the site. In an additional measure to reduce the unrealistic late-summer drought stress in the model, root distribution was adjusted based on CLM's default parameter values for the broadleaf evergreen temperate tree plant functional type, shifting roots towards deeper soil layers. The reader is referred to Appendix A for a more complete description of the parameters that were adjusted and the calibration approach used.

All model results presented and discussed in Sect. 3 are based on the optimized model.

2.7 Canopy Conductance

Observed canopy conductance (G_c, m s^{-1}) was calculated by combining hourly tower data (see Sect. 2.3) with the Penman-Monteith equation (Monteith, 1964) as in Wharton et al. (2012):

$$G_c = \left[\frac{\rho c_p \mathrm{VPD}}{\gamma LE} + \frac{\left(\frac{\Delta_{sat}}{\gamma}\right)\left(\frac{H}{LE}\right)-1}{G_a}\right]^{-1} \quad (7)$$

where ρ and c_p are the density and specific heat of air, respectively (kg m^{-3}, J kg^{-1} K^{-1}), VPD is the atmospheric vapor pressure deficit (kPa), LE is the latent heat flux (W m^{-2}), Δ_{sat} is the slope of the saturation vapor pressure curve as a function of air temperature (kPa K^{-1}), γ is the psychrometric constant (kPa K^{-1}), H is the sensible heat flux (W m^{-2}), and $G_a = u_*^2/U$ is the aerodynamic conductance for momentum transfer (m s^{-1}), where u_* is the friction velocity and U is the wind speed. Atmospheric pressure and air temperature data and the ideal gas law were later used to convert the G_c values to mmol m^{-2} s^{-1}. The calculation of G_c was restricted to daytime hours (10:00–16:00 PST) and to the months of June to September (dry season). Rain events and periods with $LE < 5$ W m^{-2} or relative humidity $> 80\%$ were disregarded. G_c values outside the interval of 0 to 1000 mmol m^{-2} s^{-1} were also disregarded.

For comparison against observations, modeled canopy conductance values were calculated using the same methodology described above, but using hourly CLM output (H, LE, u_*) instead. An alternative would be to calculate

Biogeosciences Discuss., doi:10.5194/bg-2016-441, 2016
Manuscript under review for journal Biogeosciences
Published: 21 October 2016

canopy conductance directly by upscaling CLM's leaf stomatal conductance and leaf boundary-layer conductance using leaf area index (LAI). Canopy conductance values derived from both approaches were found to be strongly correlated. The Penman-Monteith method was ultimately selected for the calculation of G_c in order to allow a more direct comparison between modeled and observed values. This comparison was done as a way to assess the performance of CLM in the simulation of leaf stomatal conductance.

3 Results and Discussion

3.1 Carbon Pools and Isotopic Signatures

Figure 2 shows modeled LAI, carbon stocks (leaf, fine root, coarse root, tree wood, and soil organic matter (SOM) carbon), and $\delta^{13}C$ of leaf and SOM pools throughout the transient run (1850–2006). Before the transient run, the model was spun-up and successfully equilibrated under the defined pre-industrial scenario, with LAI, carbon stocks, and leaf/SOM carbon isotope ratios reaching steady state (results not shown). The cyclic behavior exhibited in Fig. 2 is related to the driving meteorological data set, which was cycled throughout the simulation period (Sect. 2.5).

From 1850 to 2006, modeled LAI and carbon stocks (Fig. 2a–f) increased due to CO_2 fertilization and increasing nitrogen deposition. Average values of LAI, leaf carbon, and tree wood carbon at the end of the simulation (year 2006) were in agreement with the reference values reported in the AmeriFlux database for the Wind River site (Table 2). Modeled fine root and coarse root carbon were underestimated, but within 2 standard deviations from the reference values (Table 2).

The $\delta^{13}C$ of leaves and SOM was initialized in the model with a value of −6‰ (default value in CLM, close to the pre-industrial atmospheric $\delta^{13}CO_2$ value of −6.5‰ used in this study). During the model spin-up, in which constant pre-industrial atmospheric $\delta^{13}CO_2$ and CO_2 concentration values were prescribed, the $\delta^{13}C$ values stabilized at $\approx -26‰$. During the transient simulation (Fig. 2g), the $\delta^{13}C$ of both leaves and SOM decreased (the pools became isotopically "lighter"), mostly due to the decreasing atmospheric $\delta^{13}CO_2$ values associated with the "Suess effect" (Keeling, 1979) but also due to the increasing atmospheric CO_2 concentration values. The $\delta^{13}C$ of leaves declined faster over the years than the $\delta^{13}C$ of SOM, given the fact that leaves have a significantly shorter turnover time than SOM and therefore present a faster response to the changes in atmospheric $\delta^{13}CO_2$ and CO_2 concentration. Modeled $\delta^{13}C$ of leaves at the end of the transient simulation was within the range of site observations for mid-canopy leaves, and just 0.2‰ below the range of observations for top-canopy leaves (Table 2). Modeled $\delta^{13}C$ of SOM (top 1 m of soil) was within the range of site observations for SOM at 20 cm below ground (Table 2).

The overall agreement between the observed and modeled carbon isotope ratios indicates that the calibrated CLM had skill in simulating the balance between assimilation and stomatal conductance and the associated photosynthetic ^{13}C discrimination. The adjustment of the parameters controlling stomatal conductance in the model (m_{bb} and b_{bb} – see Sect. 2.6, Table 1 and Appendix A9) to improve the simulation of evapotranspiration had a significant impact on the simulation of photosynthetic ^{13}C discrimination. When using the default parameter values (resulting in significantly higher stomatal

Biogeosciences Discuss., doi:10.5194/bg-2016-441, 2016
Manuscript under review for journal Biogeosciences
Published: 21 October 2016

conductance values), the modeled values of $\delta^{13}C$ in leaves and SOM were generally 2–3‰ lower (Fig. A1), departing from site observations (cf. Table 2).

3.2 Energy and Carbon Fluxes

Modeled energy and carbon fluxes are compared against daily-averaged observations in Fig. 3 for the period between 1998 and 2006. "Observed" GPP and ER were obtained from applying a partitioning model to NEE measurements (Sect. 2.3), but are referred to as "observations" in the text.

Modeled LE values were close to observations, with a mean bias error (MBE) of ≈ -3 W m^{-2} and a root mean square error (RMSE) of ≈ 20 W m^{-2}. The adjustment of the stomatal conductance parameters m_{bb} and b_{bb} (Table 1) was fundamental in modifying the LE simulations. When using the default parameter values the modeled evapotranspiration was significantly overestimated, with summer values exceeding observations by almost 100% (Fig. A2a).

In 1998–2003 the model overestimated H (MBE ≈ 32 W m^{-2}, RMSE ≈ 40 W m^{-2}), while in 2004–2006 the modeled values were closer to observations (MBE ≈ 10 W m^{-2}, RMSE ≈ 36 W m^{-2}). The modeled H values did not present significant interannual variability in 1998–2006; however, the observations showed significantly smaller fluxes in 1998–2003 than in 2004–2006. Such changes in the magnitude of H were reported as a potential data issue in the Wind River site documentation available in the AmeriFlux repository.

Modeled GPP resembled observed values, with small differences (MBE ≈ 0.23 gC m^{-2} day^{-1}, RMSE ≈ 1.60 gC m^{-2} day^{-1}). Modeled ER exhibited closer correspondence with measurements during the spring and summer months in general (MBE ≈ 0.82 gC m^{-2} day^{-1}, RMSE ≈ 1.85 gC m^{-2} day^{-1}), with summer peaks especially close to measured values. In the colder months, modeled ER was significantly overestimated (MBE ≈ 1.46 gC m^{-2} day^{-1}, RMSE ≈ 1.77 gC m^{-2} day^{-1}).

Despite the significant improvement in the seasonal behavior of ER after the Q_{10} adjustments discussed in Sect. A6, the results indicate that further adjustments also including the base rate of maintenance respiration and the base decomposition rates for each litter and SOM pool within CLM would be necessary to better simulate the observed ER at Wind River. The results suggest that lower base rates and higher Q_{10} values would improve the simulations at the site.

3.3 Isotopic Signatures of GPP and ER

3.3.1 Diurnal Cycle

Modeled $\delta^{13}C_{GPP}$ exhibited a well-defined diurnal cycle (Fig. 4), with minimum values in the early morning and late afternoon and a peak value typically in mid-afternoon, reflecting diurnal changes in the simulated iWUE (see Eqs. 4 and 6). Modeled $\delta^{13}C$ values of the heterotrophic component of ecosystem respiration (HR) were approximately constant, with a ≈ 0.2‰ change over the entire period of study (1998–2006). On the other hand, modeled $\delta^{13}C$ values of the autotrophic component (AR) were found to be virtually equal to modeled $\delta^{13}C_{GPP}$ during daytime. At nighttime, modeled $\delta^{13}C_{AR}$ was

Biogeosciences Discuss., doi:10.5194/bg-2016-441, 2016
Manuscript under review for journal Biogeosciences
Published: 21 October 2016

found to change abruptly towards values closer to modeled $\delta^{13}C_{HR}$. Because AR was the major component of the total ecosystem respiration (ER=AR+HR; see Fig. 4a), modeled $\delta^{13}C_{ER}$ exhibited a similar behavior compared to modeled $\delta^{13}C_{AR}$ (Fig. 4b).

In CLM, newly assimilated carbon is first allocated to meet the total maintenance respiration demand of live plant tissues (top priority). When this demand exceeds the supply of carbon via photosynthesis (e.g., during nocturnal periods, wintertime, stress periods), carbon is drawn from a storage pool (excess maintenance respiration pool; CS_{xs}), which is allowed to run a deficit state. The reason CLM allows this deficit state is to avoid the requirement of knowing the size of the total storage pool available to plants and thus the possibility of vegetation dying in a given location if the storage pool is depleted, because, without vegetation dynamics active there would not be the possibility of recruiting new vegetation. When negative, CS_{xs} is gradually replenished with newly assimilated carbon at a potential rate of $-CS_{xs}/(86400\tau_{xs})$, where τ_{xs} is a time constant (set to 30 days in CLM). The carbon allocation flux to replenish CS_{xs} receives second priority in the model, while the carbon allocation fluxes to support plant growth have third priority. Given this allocation structure, $\delta^{13}C_{MR}$ (maintenance respiration) is expected to follow $\delta^{13}C_{GPP}$ during daytime (assuming GPP is enough to meet the MR demand), and the $\delta^{13}C$ of the CS_{xs} pool during nighttime. Also, the $\delta^{13}C$ of the CS_{xs} pool is expected to have little sensitivity to recent photosynthetic ^{13}C discrimination, given the rate at which the pool is refilled. The simulations results in Fig. 4b align with these expectations.

Autotrophic respiration at Wind River is likely fueled by a mixture of stored and recently-fixed carbon, as indicated by ^{14}C measurements from root respiration at the site (Taylor et al., 2015). This process cannot be appropriately modeled by CLM with the current carbon allocation scheme, impacting the simulation of $\delta^{13}C_{ER}$. An explicit representation of carbohydrate storage pools within CLM to support the maintenance respiration demand would improve the simulation of $\delta^{13}C_{ER}$. The need for a better representation of carbohydrate storage pools within CLM was also highlighted by the $^{13}CO_2$-labeling study conducted by Mao et al. (2016).

3.3.2 Seasonal Cycle

As illustrated in Fig. 5, modeled $\delta^{13}C_{GPP}$ exhibited a well-defined seasonal pattern, peaking during the summer as a result of a decrease in the photosynthetic ^{13}C discrimination associated with higher iWUE values (see Eqs. 4 and 6). The summer peak in iWUE was linked to changes in stomatal conductance in response to increased VPD and reduced SWC associated with summer drought.

On a monthly scale, roughly indicated by the smoothed curve in Fig. 5, the modeled $\delta^{13}C_{GPP}$ values presented a similar seasonal pattern in comparison with the $\delta^{13}C_{ER}$ observations at the site by Lai et al. (2005). Differences between $\delta^{13}C_{GPP}$ and $\delta^{13}C_{ER}$ are obviously expected, as $\delta^{13}C_{ER}$ depends on the contribution of recently-assimilated carbon to AR, the AR:ER ratio, and also post-photosynthetic fractionation (Bowling et al., 2008; Brüggemann et al., 2011). The seasonal pattern in the observed $\delta^{13}C_{ER}$ (Fig. 5) could be partially attributed to an eventual spring-to-summer decrease in AR:ER ratio (assuming $\delta^{13}C_{HR} > \delta^{13}C_{AR}$). ^{14}C measurements from below-ground respiration components at Wind River reported by

Biogeosciences Discuss., doi:10.5194/bg-2016-441, 2016
Manuscript under review for journal Biogeosciences
Published: 21 October 2016

Taylor et al. (2015) do indicate a spring-to-summer decrease in the contribution of root respiration (RR) towards total soil respiration (SR=RR+HR). The similarity of the seasonal patterns of observed $\delta^{13}C_{ER}$ and modeled $\delta^{13}C_{GPP}$ suggests that stomatal response to drought could also be driving the seasonal pattern in the observed $\delta^{13}C_{ER}$ at the site. The broader implication is that $\delta^{13}C_{ER}$, which can be more easily measured than $\delta^{13}C_{GPP}$, can be reasonably used as a surrogate to indicate forest response to drought at Wind River.

Due to the limitations in the carbon allocation scheme used in CLM (Sect. 3.3.1), the simulated $\delta^{13}C_{ER}$ values were found to be inconsistent with the site observations, with nocturnal values approximately constant throughout the entire period of study (1998–2006), exhibiting little sensitivity to recent photosynthetic ^{13}C discrimination. Diurnal values, on the other hand, were found to be strongly correlated with $\delta^{13}C_{GPP}$, given the fact that in CLM current photosynthate directly fuels AR (results not shown).

The adjustment of the stomatal conductance parameters m_{bb} and b_{bb} to improve the simulation of evapotranspiration (Sect. 2.6, Table 1 and Appendix A9) led to a significant change in the simulation of $\delta^{13}C_{GPP}$. When the default parameter values were used, modeled $\delta^{13}C_{GPP}$ was generally 2–3‰ lower due to higher photosynthetic ^{13}C discrimination (Fig. A2b), also presenting a considerable reduction in the amplitude of the seasonal cycle. The difference between modeled $\delta^{13}C_{GPP}$ and observed $\delta^{13}C_{ER}$ was significantly larger. As discussed in Sect. 3.1, site observations of leaf and SOM $\delta^{13}C$ support the notion that the default stomatal conductance parameters are inadequate at Wind River, resulting in excessive photosynthetic ^{13}C discrimination.

Thanks to the recent implementation of photosynthetic ^{13}C discrimination within CLM, the results of the present study indicate that $\delta^{13}C$ data can be used to constrain stomatal conductance and iWUE in the model as an alternative to eddy covariance flux measurements. This new capability in CLM also opens an interesting opportunity for future model developments, as isotopes expose a conceptual weakness in CLM's carbon allocation scheme (the deficit-based accounting scheme described in Sect. 3.3.1). In future efforts, $\delta^{13}C_{ER}$ data can be used to guide a restructuring of the model, moving away from the deficit-based accounting scheme towards an explicit representation of carbohydrate storage pools.

3.4 Ecosystem Drought Response

Throughout the simulation period (1998–2006), the calibrated CLM predicted a few periods where the ecosystem was under the influence of drought stress (Fig. 6). As indicated by the β_t parameter (Eq. 3), which varies from 0 (maximum drought stress) to 1 (no drought stress) (see Sect. 2.1), those periods included the summers of 1998, 2006, 2003, and 2002, in decreasing order of drought severity. The departures from $\beta_t = 1$ typically occurred when modeled SWC (top 5 soil layers, 0–27 cm) decreased below $\approx 20\%$.

After the adjustment of soil hydrology parameters (Sect. A7), CLM was able to adequately simulate SWC throughout most of the years within the study period (Fig. 6), especially during the summer months, with an overall summer MBE of 3.24%. However, the simulated SWC significantly departed from observations in 1999–2002. CLM, which was driven by observed precipitation at the site, indicated higher SWC than observations in 1999–2002, particularly during the

Biogeosciences Discuss., doi:10.5194/bg-2016-441, 2016
Manuscript under review for journal Biogeosciences
Published: 21 October 2016

summer months, with a summer MBE of 8.05%. For the remaining years, summer MBE was −0.27%. The SWC observations starting on the second year of the site records (1999) up to the data gap in 2002 presented a different pattern in comparison with the remaining years, showing an apparent negative offset of near 10%. It is likely that the apparent shift in the time series of observed SWC was instrument-related. In 1999–2002, soil moisture monitoring at the site consisted of 2, 2-pronged TDR probes instead of 6, 3-pronged TDR probes, likely resulting in less-accurate data collection.

Observed canopy conductance was found to be strongly dependent on VPD, following a decreasing exponential relationship (Fig. 7). In order to investigate the additional dependence on drought stress, the data points were divided into 4 bins according to the observed values of SWC (Fig. 7a). The linear regression fit between $\log G_c$ and VPD for the points corresponding to the lowest SWC bin (SWC<17.5%, $\approx 22\%$ of all data points) was virtually the same as the linear regression considering all data points. If the forest were under drought stress at those low SWC levels, the former regression curve with data points from the lowest SWC bin would be expected to be found below the latter. Instead, the SWC<17.5% regression curve was very similar—even slightly above the regression curve using all data points.

As discussed above, the observed SWC values in 1999–2002 were suspected to have a negative bias, i.e., drier than reality. G_c values in Fig. 7a corresponding to the summer of 1999–2002 were tagged as belonging to the lowest SWC bin, but in reality, they could be associated with wetter, non-drought-stress conditions. Assuming CLM's summer simulated SWC (driven by observed precipitation) was not as biased as the observed SWC might be, we instead used the modeled SWC values to probe the G_c vs. VPD relationship under different SWC regimes in Fig. 7b. Interestingly, with this approach, a distinct pattern emerged for the data points within the lowest SWC bin. The regression curve considering all data points was $\log G_c = -0.59\text{VPD} + 6.06$ ($r = -0.60$) and when considering only the data points from the lowest bin (modeled SWC<21.25%, $\approx 24\%$ of all points), the regression curve was $\log G_c = -0.50\text{VPD} + 5.71$ ($r = -0.56$). The latter regression curve corresponded to reasonably lower G_c values, especially at low VPD levels, which is compatible with a drought stress scenario. The result supports the suspicion of a negative bias in the observed SWC data in 1999–2002.

Similar to observations, modeled canopy conductance was also found to be strongly dependent on VPD (Fig. 8). This is expected given the Ball-Berry stomatal conductance model used in CLM (Eq. 2). The Ball-Berry model has a direct dependence on leaf relative humidity (leaf RH), not leaf VPD, but these variables are strongly correlated. The correlation between modeled G_c and RH was found to be slightly higher than between modeled G_c and VPD, while observed G_c correlated slightly better with VPD than RH (results not shown). The results indicate that a direct dependence on leaf VPD in CLM's stomatal conductance model, rather than leaf RH, would lead to a more accurate representation of stomatal functioning at Wind River, but overall, such improvement is expected to be small. The general dependence of modeled canopy conductance on VPD was very similar in comparison with observations, as indicated by the linear regression curve between $\log G_c$ and VPD in Fig. 8 using all data points ($\log G_c = -0.59\text{VPD} + 6.04$; compare with $\log G_c = -0.59\text{VPD} + 6.06$ in Fig. 7b). The correlation between observed $\log G_c$ and VPD, however, was lower than for the model results ($r = -0.60$ and $r = -0.91$, respectively).

Biogeosciences Discuss., doi:10.5194/bg-2016-441, 2016
Manuscript under review for journal Biogeosciences
Published: 21 October 2016

The impact of drought stress on modeled G_c is clearly visible in Fig. 8a, in which the data points were binned according to β_t. With increasing drought stress (decreasing β_t values), the modeled G_c values still maintained a strong dependence on VPD, but were shifted downward, particularly at low VPD levels. In order to allow a more direct comparison between the impact of drought stress on modeled and observed canopy conductance, the data points were separated according to modeled SWC in Fig. 8b. The points in the lowest SWC bin (SWC<21.25%, ≈ 22% of all points) roughly corresponded to the periods under drought stress ($\beta_t < 1$). The regression curve for the SWC<21.25% group laid reasonably below the regression curve considering all data points ($\log G_c = -0.53\text{VPD} + 5.80$, $r = -0.90$ and $\log G_c = -0.59\text{VPD} + 6.04$, $r = -0.91$, respectively). The regression curves associated with SWC<21.25% were similar for the observed and modeled results (Figs. 7b and 8b), but apparently indicated a small underestimation of drought stress in CLM (i.e., a small overestimation of G_c; note the G_c intercepts at 301 and 331 mmol m^{-2} s^{-1} in Figs. 7b and 8b, respectively). It is important to point out, however, that modeled SWC was used to segregate the observations in Fig. 7b.

Modeled $\delta^{13}C_{GPP}$ and G_c were highly correlated ($r = -0.88$, $p < 0.001$; Fig. 9b). Modeled G_c generally decreased into the summer season, leading to an increase in water use efficiency and a decrease in photosynthetic ^{13}C discrimination, resulting in higher $\delta^{13}C_{GPP}$ values. Observed $\delta^{13}C_{ER}$ was found to have a low negative correlation with observed G_c, but not statistically significant ($r = -0.27$, $p = 0.396$; Fig. 9a). The low correlation was likely a result of $\delta^{13}C_{ER}$ reflecting constraints of prior environmental drivers in comparison with the more rapid response of G_c to more recent environmental drivers. Another possible explanation is that the monthly $\delta^{13}C_{ER}$ values in Fig. 9a were obtained by averaging up to 4 discrete weekly observations (see Sect. 2.4), in contrast with the calculation of monthly G_c, which used daytime values for each day of the month. It is important to mention that the observed $\delta^{13}C_{ER}$ do show a clear seasonal pattern (Fig. 5), with values peaking during summer likely in response to changes in g_s and iWUE associated with summer drought (see discussion in Sect. 3.3.2), but the present results indicate a lag in this response.

4 Conclusions

After a substantial calibration of model parameters, CLM was able to simulate energy and carbon fluxes, leaf area index, and carbon stocks at an old-growth coniferous forest (Wind River AmeriFlux site) in general agreement with site observations. Overall, the calibrated CLM was able to simulate the observed response of canopy conductance to atmospheric vapor pressure deficit and soil water content, reasonably capturing the impact of drought stress on ecosystem functioning. Key model adjustments to simulate observed flux and carbon stock patterns included *i*) parameters controlling the variation of specific leaf area through the forest canopy (SLA_0, m), with significant impact on GPP, *ii*) parameters controlling stomatal conductance (m_{bb}, b_{bb}), with significant impact on the simulated latent heat flux, and *iii*) soil hydraulic parameters, with impact on soil water content and on the drought stress parameter, β_t. The calibrated parameters presented here may be of use for future modeling studies involving stands of similar age and composition under a similar climate regime. More broadly, the calibration of the Ball-Berry stomatal conductance parameters aligned with observations reported in the

Biogeosciences Discuss., doi:10.5194/bg-2016-441, 2016
Manuscript under review for journal Biogeosciences
Published: 21 October 2016

literature for coniferous trees, suggesting that a future release of CLM would benefit from using a distinct, lower slope value ($m_{bb} = 6$) for conifers, rather than a unique value for all C3 plants ($m_{bb} = 9$).

The calibrated CLM was able to simulate carbon isotope ratios of leaves and soil organic matter at Wind River, in general agreement with site observations. The adjustments made on the parameters controlling stomatal conductance within the model, originally aiming to improve the simulation of evapotranspiration, were critical to simulate the observed photosynthetic ^{13}C discrimination at the site. The simulation of nocturnal $\delta^{13}C_{ER}$ was found to be inconsistent with site observations, with results showing little sensitivity to recent photosynthetic ^{13}C discrimination. The inclusion of explicit carbohydrate storage pools within CLM (and removal of the current deficit-based carbon accounting system) to support the maintenance respiration demand from live plant tissues would improve the simulation of $\delta^{13}C_{ER}$. The optimized model also tended to overestimate ecosystem respiration through the winter, suggesting further investigation of the respiration-temperature relationships and perhaps also changes in physiological activity of leaves and fine roots through the winter.

The recent inclusion of the photosynthetic ^{13}C discrimination functionality in CLM opens a new opportunity for model testing. The results presented here indicate that $\delta^{13}C$ data can be used to constrain stomatal conductance and iWUE in the model, as an alternative to eddy covariance flux measurements. Also, this new functionality in CLM opens an interesting opportunity for future model developments, as isotopes expose a conceptual weakness in CLM's carbon allocation scheme (the deficit-based accounting system). In future efforts, $\delta^{13}C_{ER}$ data can be used to guide a restructuring of the model, moving away from the deficit-based accounting scheme towards an explicit representation of carbohydrate storage pools.

Appendix A: CLM Calibration

Most of the adjustments were performed on parameters particular to the needleleaf evergreen temperate tree plant functional type in CLM. For brevity, this plant functional type is referred to as NETT PFT in the following Sections.

A1 Carbon Allocation Ratios

By default, CLM uses a dynamic new-stem-carbon-to-new-leaf-carbon allocation ratio ($A_{s:l}$, gC gC^{-1}) for the NETT PFT, which rises with increasing net primary production. A survey by White et al. (2000) indicates an average $A_{s:l}$ of 2.2 ± 0.89 gC gC^{-1} for needleleaf evergreen forests. Measurements reported by Hudiburg et al. (2013) for a region close to the Wind River site and characterized by forests of similar species composition vary approximately between 1 and 3.5 gC gC^{-1} (their Fig. A1 – Mesic sites). A fixed value of $A_{s:l} = 2$ gC gC^{-1} (value also used by Thornton et al., 2002 in their BIOME-BGC simulations for the Wind River site) was found to improve the simulated forest biomass and was adopted in this study for the NETT PFT.

The new-fine-root-carbon-to-new-leaf-carbon allocation ratio parameter ($A_{fr:l}$, gC gC^{-1}) for the NETT PFT was also changed based on observations at the Wind River site reported in the AmeriFlux database indicating $A_{fr:l} = 0.385$

Biogeosciences Discuss., doi:10.5194/bg-2016-441, 2016
Manuscript under review for journal Biogeosciences
Published: 21 October 2016

gC gC^{-1} rather than the default value of 1 gC gC^{-1}. The change meant a significantly greater carbon investment to leaves, helping to increase the modeled GPP towards the site observations.

A2 Carbon:Nitrogen Ratios

Leaf-litter C:N ratio (CN_{llit}, gC gN^{-1}) for the NETT PFT was adjusted based on measurements at the Wind River site (Klopatek, 2007) to 76.4 gC gN^{-1} (mean observed value). Based on the mean observed CN_{llit} and assuming a nitrogen retranslocation efficiency of 50% (survey by Parkinson, 1983 indicates efficiencies around 50% for conifer trees and 36–69% for Douglas-fir in particular), the leaf C:N ratio (CN_l, gC gN^{-1}) for NETT PFT was adjusted to 38.2 gC gN^{-1}. The updated parameters differ little from the default values ($CN_{llit} = 70$ gC gN^{-1}, $CN_l = 35$ gC gN^{-1}).

Fine-root C:N ratio (CN_{fr}, gC gN^{-1}) for the NETT PFT was also adjusted based on measurements at the Wind River site (Klopatek, 2007). The value was adjusted from 42 gC gN^{-1} (default) to 64.7 gC gN^{-1} (mean observed value), meaning a significantly smaller nitrogen investment in fine roots resulting in more nitrogen for investment in leaves. This change helped to increase the modeled GPP towards the site observations.

A3 Leaf Longevity

Measurements reported by Hudiburg et al. (2013) for a region near the Wind River site and characterized by forests of similar species composition indicate leaf longevity (τ_l) of 5 yrs. This value was adopted for the NETT PFT, replacing the default value of 3 yrs. This change contributed particularly to an increase in the modeled leaf area index.

A4 Specific Leaf Area

In CLM, specific leaf area (SLA, m^2 leaf gC^{-1}) is assumed to be linear with canopy depth x (expressed as overlying leaf area index, m^2 leaf m^{-2} ground) (Thornton and Zimmermann, 2007):

$$\mathrm{SLA}(x) = \mathrm{SLA}_0 + mx \quad \text{(A1)}$$

where SLA_0 is the specific leaf area at the top of canopy and m is a linear coefficient (m^2 ground gC^{-1}). Integrating this equation over the canopy, a relationship can be established where leaf area index (LAI, m^2 leaf m^{-2} ground) is calculated as a function of leaf carbon (C_l, gC m^{-2} ground), knowing the parameters SLA_0 and m (Thornton and Zimmermann, 2007):

$$\mathrm{LAI} = \frac{\mathrm{SLA}_0\left(e^{mC_l}-1\right)}{m} \quad \text{(A2)}$$

The default NETT PFT values in CLM for SLA_0 and m are 0.01 m^2 leaf gC^{-1} and 0.00125 m^2 ground gC^{-1}, respectively. These values were found to be too large for the Wind River site. Using them in Eq. (A2) with a C_l of 941 gC m^{-2} ground (mean observation at the Wind River site reported in the AmeriFlux database) results in an LAI of ≈ 18 m^2 leaf m^{-2} ground, instead of ≈ 9 m^2 leaf m^{-2} ground according to the observations at the Wind River site (AmeriFlux database).

Biogeosciences Discuss., doi:10.5194/bg-2016-441, 2016
Manuscript under review for journal Biogeosciences
Published: 21 October 2016

In CLM, the maximum rate of carboxylation at 25°C (V_{cmax25}) is proportional to the area-based leaf nitrogen concentration defined as $N_a = 1/(CN_l \mathrm{SLA}_0)$, i.e., $V_{cmax25} \propto 1/\mathrm{SLA}_0$. Using the default NETT PFT values for SLA_0 and m led to the development of large and thin leaves with reduced N_a and V_{cmax25}, resulting in excessive LAI and significant down-regulation of GPP. Smaller SLA_0 values were attempted, with m values constrained by Eq. (A2), the SLA_0 value, and the site observations of LAI and C_l mentioned above, aiming to minimize model errors in the simulation of GPP and LAI. $\mathrm{SLA}_0 = 0.006$ m^2 leaf gC^{-1} and $m = 0.000985$ m^2 ground gC^{-1} were found to significantly improve the simulations and were adopted instead of the default values. Measurements reported by Woodruff et al. (2004) indicate that the ratio of leaf dry mass to leaf area reaches 263 g m^{-2} leaf near the canopy top at Wind River (their Fig. 6). Assuming the mass of carbon is 50% of the dry mass, the observed value corresponds to 131.5 gC m^{-2} leaf, i.e., an SLA_0 value of 0.0076 m^2 leaf gC^{-1}, indicating that the optimized SLA_0 value moved in the right direction from the default NETT PFT value (0.0100 down to 0.0060 m^2 leaf gC^{-1}), but ended up slightly lower than the observed value.

A5 Tree Mortality

Results reported by van Mantgem et al. (2009) indicate an increasing trend of plant mortality rates (M, yr^{-1}) for Pacific Northwest forests, with M growing from ≈ 1% yr^{-1} in 2000 towards ≈ 1.5% yr^{-1} in 2010. In CLM, a default rate of $M = 2\%$ yr^{-1} is used for all vegetation types, which was found to be excessive at Wind River, leading to a reduced modeled forest biomass. $M = 1.5\%$ yr^{-1} was found to yield results closer to site observations and was therefore adopted in this study.

A6 Temperature Sensitivity Coefficient (Q_{10})

The effect of temperature on maintenance respiration (component of autotrophic respiration) in CLM is calculated via a Q_{10} formulation, where the base rate of maintenance respiration is multiplied by $Q_{10}^{(T_a - T_{ref})/10}$, where Q_{10} is a temperature sensitivity coefficient, T_a is air temperature, and T_{ref} is a reference temperature. For the maintenance respiration cost for live fine roots, soil temperature at the respective soil layer ($T_{s,i}$) is used instead of T_a. Similarly, the effect of temperature on decomposition (and therefore on heterotrophic respiration) is also calculated via a Q_{10} formulation, where the base rates of decomposition are multiplied by $Q_{10}^{(T_{s,i} - T_{ref})/10}$. In CLM, a default Q_{10} of 1.5 is used for both maintenance respiration and decomposition. However, nighttime CO_2 flux measurements above the canopy at Wind River, which would include the sum of autotrophic and heterotrophic respiration, indicate a Q_{10} of 2.49 (Misson et al., 2007). By adjusting CLM's Q_{10} to 2.5 for both maintenance respiration and decomposition, the seasonal behavior of ecosystem respiration better corresponded with observed values. This was especially the case for heterotrophic respiration, reducing the model overestimation during winter and the model underestimation during summer.

Biogeosciences Discuss., doi:10.5194/bg-2016-441, 2016
Manuscript under review for journal Biogeosciences
Published: 21 October 2016

A7 Soil Hydraulic Properties

Initial runs indicated poor performance of CLM in the simulation of soil water content at the Wind River site (strong dry bias), which resulted in an unrealistic down-regulation of GPP due to drought stress late in the dry, summer season. When using the original soil hydraulic properties from CLM v.4.0 the results were greatly improved, with a wetter soil and a reduction of the unrealistic drought effect. The observed improvement was likely related to a smaller subsurface runoff in CLM v.4.0 and consequently greater water retention in the soil. In CLM, subsurface runoff is proportional to a term representing the maximum drainage when the water table depth is at the surface (q_{drai}^{max}). In CLM v.4.0, $q_{drai}^{max} = 0.0055$ kg m^{-2} s^{-1}, while in CLM v.4.5 $q_{drai}^{max} = 10 \sin\beta$ kg m^{-2} s^{-1}, where β is the mean grid cell topographic slope. Even for a small 1° slope, q_{drai}^{max} is significantly larger than in CLM v.4.0 (0.1745 kg m^{-2} s^{-1}). The soil hydraulic properties from CLM v.4.0 were therefore used in this study.

A8 Root Distribution

In CLM, root distribution over soil depth is calculated as (Oleson et al., 2013):

$$r_i = 0.5(e^{-r_a z_{h,i-1}} + e^{-r_b z_{h,i-1}}) - 0.5\alpha(e^{-r_a z_{h,i}} + e^{-r_b z_{h,i}}) \quad \text{(A3)}$$

where r_i is the root fraction at the soil layer i, $z_{h,i}$ (m) is the depth from the soil surface to the interface between layers i and $i+1$ ($z_{h,0} = 0$ corresponds to the soil surface), r_a and r_b are root distribution parameters (m^{-1}), $\alpha = 1$ for $1 \leq i < N_{levsoi}$, and $\alpha = 0$ for $i = N_{levsoi}$ (N_{levsoi} is the number of soil layers). The sum of r_i over the whole soil column is equal to 1. Root fraction in combination with a plant wilting factor w_i (function of soil water potential and a plant-dependent response to drought stress) are used to calculate an integrated drought stress parameter in CLM, β_t, which downregulates stomatal conductance in the model (see Sect. 2.1; Eqs. 2 and 3).

The default root distribution parameters for the NETT PFT are $r_a = 7$ m^{-1} and $r_b = 2$ m^{-1}. In this study r_b for the NETT PFT was changed to 1 m^{-1} (default CLM value for broadleaf evergreen temperate tree plant functional type), shifting roots towards deeper soil layers, in order to make water stored at deeper soil layers available to the trees and, along with the changes in the soil hydraulic properties discussed in Sect. A7, minimize the model overestimation of drought stress at the Wind River site during late summer.

A9 Stomatal Conductance

In CLM, leaf stomatal conductance is calculated based on the Ball-Berry model as described by Collatz et al. (1991) and implemented by Sellers et al. (1996) in the SiB2 model (see Eq. 2). The default values set for the parameters m_{bb} and b_{bb} in CLM for C3 plants (9 and 10 mmol m^{-2} leaf s^{-1}, respectively) were found to be inadequate at Wind River, leading to a significant overestimation of latent heat fluxes due to excessive plant transpiration (after the adjustments discussed in the aforementioned Sections which resulted in higher forest productivity). These default parameter values were established based on the values used in the SiB2 model (Sellers et al., 1996). In SiB2, however, a distinction was made for coniferous

Biogeosciences Discuss., doi:10.5194/bg-2016-441, 2016
Manuscript under review for journal Biogeosciences
Published: 21 October 2016

forests ($m_{bb} = 6$) but was not carried over to CLM. Observations reported in the literature support this lower m_{bb} value for conifers (see for example the survey by Williams et al., 2004, Table 6.3). On the other hand, b_{bb} values reported in the literature are highly variable (1–400 mmol m^{-2} leaf s^{-1} in the survey by Barnard and Bauerle, 2013 for a broad range of plant species). In CLM v.4.0, the default b_{bb} for C3 plants is significantly smaller than in CLM v.4.5 (2 vs. 10 mmol m^{-2} leaf s^{-1}) (Oleson et al., 2010). $m_{bb} = 6$ and $b_{bb} = 5$ mmol m^{-2} leaf s^{-1} were found to greatly improve the modeled latent heat fluxes at the Wind River site, and were therefore adopted in this study. The updated values also resulted in a great improvement in the simulation of $\delta^{13}C$ of leaves, SOM, and GPP. Figures A1 and A2 illustrate the impact of the stomatal conductance parameters on model performance, particularly in regards to latent heat fluxes and photosynthetic ^{13}C discrimination.

Acknowledgments

This research was supported by the U.S. Department of Energy's Office of Science, Terrestrial Ecosystem Science Program, Grant ER65543. PET was supported by the U.S. Department of Energy's Office of Science, Biological and Environmental Research, Accelerated Climate Modeling for Energy project. We acknowledge the Wind River Field Station AmeriFlux site (US-Wrc, PIs: Kenneth Bible, Sonia Wharton) for its data records. Funding for AmeriFlux data resources was provided by the U.S. Department of Energy's Office of Science. Data and logistical support were also provided by the U.S. Forest Service Pacific Northwest Research Station.

References

Baldocchi, D., Falge, E., Gu, L., Olson, R., Hollinger, D., Running, S., Anthoni, P., Bernhofer, C., Davis, K., Evans, R., Fuentes, J., Goldstein, A., Katul, G., Law, B., Lee, X., Malhi, Y., Meyers, T., Munger, W., Oechel, W., Paw U, K. T., Pilegaard, K., Schmid, H. P., Valentini, R., Verma, S., Vesala, T., Wilson, K., and Wofsy, S.: FLUXNET: a new tool to study the temporal and spatial variability of ecosystem-scale carbon dioxide, water vapor, and energy flux densities, B. Am. Meteorol. Soc., 82, 2415–2434, 2001.

Barnard, D. M. and Bauerle, W. L.: The implications of minimum stomatal conductance on modeling water flux in forest canopies, J. Geophys. Res.-Biogeo., 118, 1322–1333, 2013.

Barr, A., Ricciuto, D., Schaefer, K., Richardson, A., Agarwal, D., Thornton, P., Davis, K., Jackson, B., Cook, R., Hollinger, D., Van Ingen, C., Amiro, B., Andrews, A., Arain, M., Baldocchi, D., Black, T., Bolstad, P., Curtis, P., Desai, A., Dragoni, D., Flanagan, L., Gu, L., Katul, G., Law, B., Lafleur, P., Margolis, H., Matamala, R., Meyers, T., McCaughey, J., Monson, R., Munger, J., Oechel, W., Oren, R., Roulet, N., Torn, M., and Verma, S.: NACP site: tower meteorology, flux observations with uncertainty, and ancillary data, ORNL Distributed Active Archive Center, doi:10.3334/ORNLDAAC/1178, 2013.

Boisvenue, C. and Running, S. W.: Simulations show decreasing carbon stocks and potential for carbon emissions in Rocky Mountain forests over the next century, Ecol. Appl., 20, 1302–1319, 2010.

Bowling, D. R., Pataki, D. E., and Randerson, J. T.: Carbon isotopes in terrestrial ecosystem pools and CO_2 fluxes, New Phytol., 178, 24–40, 2008.

Brüggemann, N., Gessler, A., Kayler, Z., Keel, S. G., Badeck, F., Barthel, M., Boeckx, P., Buchmann, N., Brugnoli, E., Esperschütz, J., Gavrichkova, O., Ghashghaie, J., Gomez-Casanovas, N., Keitel, C., Knohl, A., Kuptz, D., Palacio, S., Salmon, Y., Uchida, Y., and Bahn, M.: Carbon allocation and carbon isotope fluxes in the plant-soil-atmosphere continuum: a review, Biogeosciences, 8, 3457–3489, 2011.

Burke, E. J., Brown, S. J., and Christidis, N.: Modeling the recent evolution of global drought and projections for the twenty-first century with the Hadley Centre Climate Model, J. Hydrometeorol., 7, 1113–1125, 2006.

Collatz, G. J., Ball, J. T., Grivet, C., and Berry, J. A.: Physiological and environmental regulation of stomatal conductance, photosynthesis and transpiration: a model that includes a laminar boundary layer, Agr. Forest Meteorol., 54, 107–136, 1991.

Dai, A.: Increasing drought under global warming in observations and models, Nature Climate Change, 3, 52–58, 2013.

Damour, G., Simonneau, T., Cochard, H., and Urban, L.: An overview of models of stomatal conductance at the leaf level, Plant Cell Environ., 33, 1419–1438, 2010.

Farquhar, G. D. and Richards, R. A.: Isotopic composition of plant carbon correlates with water-use efficiency of wheat genotypes, Aust. J. Plant Physiol., 11, 539–552, 1984.

Farquhar, G. D., Ehleringer, J. R., and Hubick, K. T.: Carbon isotope discrimination and photosynthesis, Annu. Rev. Plant Phys., 40, 503–537, 1989.

Fessenden, J. E. and Ehleringer, J. R.: Temporal variation in $\delta^{13}C$ of ecosystem respiration in the Pacific Northwest: links to moisture stress, Oecologia, 136, 129–136, 2003.

Francey, R. J., Allison, C. E., Etheridge, D. M., Trudinger, C. M., Enting, I. G., Leuenberger, M., Langenfelds, R. L., Michel, E., and Steele, L. P.: A 1000-year high precision record of $\delta^{13}C$ in atmospheric CO_2, Tellus B, 51, 170–193, 1999.

Hudiburg, T. W., Law, B. E., and Thornton, P. E.: Evaluation and improvement of the Community Land Model (CLM4) in Oregon forests, Biogeosciences, 10, 453–470, 2013.

Keeling, C. D.: The Suess effect: ^{13}Carbon-^{14}Carbon interrelations, Environ. Int., 2, 229–300, 1979.

Keeling, C. D., Piper, S. C., Bacastow, R. B., Wahlen, M., Whorf, T. P., Heimann, M., and Meijer, H. A.: Atmospheric CO_2 and $^{13}CO_2$ exchange with the terrestrial biosphere and oceans from 1978 to 2000: observations and carbon cycle implications, in: A history of atmospheric CO_2 and its effects on plants, animals, and ecosystems, Ecological Studies, 177, Ehleringer, J. R., Cerling, T. E., and Dearing, M. D. (Eds.), Springer Science and Business Media Inc., New York, USA, 83–113, 2005.

Klopatek, J. M.: Litterfall and fine root biomass contribution to nutrient dynamics in second- and old-growth Douglas-fir ecosystems, Plant Soil, 294, 157–167, 2007.

Kluzek, E.: CESM research tools: CLM4.5 in CESM1.2.0 user's guide documentation, available at: http://www.cesm.ucar.edu/, 2013.

Lai, C.-T., Ehleringer, J. R., Schauer, A. J., Tans, P. P., Hollinger, D. Y., Paw U, K. T., Munger, J. W., and Wofsy, S. C.: Canopy-scale delta13C of photosynthetic and respiratory CO_2 fluxes: observations in forest biomes across the United States, Global Change Biol., 11, 633–643, 2005.

Mao, J., Ricciuto, D. M., Thornton, P. E., Warren, J. M., King, A. W., Shi, X., Iversen, C. M., and Norby, R. J.: Evaluating the Community Land Model in a pine stand with shading manipulations and $^{13}CO_2$ labeling, Biogeosciences, 13, 641–657, 2016.

Meinshausen, M., Smith, S. J., Calvin, K. V., Daniel, J. S., Kainuma, M. L. T., Lamarque, J.-F., Matsumoto, K., Montzka, S. A., Raper, S. C. B., Riahi, K., Thomson, A. M., Velders, G. J. M., and van Vuuren, D.: The RCP greenhouse gas concentrations and their extension from 1765 to 2300, Climatic Change, 109, 213–241, 2011.

Misson, L., Baldocchi, D. D., Black, T. A., Blanken, P. D., Brunet, Y., Curiel Yuste, J., Dorsey, J. R., Falk, M., Granier, A., Irvine, M. R., Jarosz, N., Lamaud, E., Launiainen, S., Law, B. E., Longdoz, B., Loustau, D., McKay, M., Paw U, K. T., Vesala, T., Vickers, D., Wilson, K. B., and Goldstein, A. H.: Partitioning forest carbon fluxes with overstory and understory eddy-covariance measurements: a synthesis based on FLUXNET data, Agr. Forest Meteorol., 144, 14–31, 2007.

Monteith, J. L.: Evaporation and environment, in: The state and movement of water in living organisms, 19th Symposium of the Society on Experimental Biology, Academic Press, New York, USA, 205–234, 1964.

Oleson, K. W., Lawrence, D. M., Bonan, G. B., Flanner, M. G., Kluzek, E., Lawrence, P. J., Levis, S., Swenson, S. C., Thornton, P. E., Dai, A., Decker, M., Dickinson, R., Feddema, J., Heald, C. L., Hoffman, F., Lamarque, J.-F., Mahowald, N., Niu, G.-Y., Qian, T., Randerson, J., Running, S., Sakaguchi, K., Slater, A., Stöckli, R., Wang, A., Yang, Z.-L., Zeng, X., and Zeng, X.: Technical description of version 4.0 of the Community Land Model (CLM), NCAR Earth System Laboratory – Climate and Global Dynamics Division, Boulder, Colorado, Tech. Rep. TN-478+STR, 2010.

Oleson, K. W., Lawrence, D. M., Bonan, G. B., Drewniak, B., Huang, M., Koven, C. D., Levis, S., Li, F., Riley, W. J., Subin, Z. M., Swenson, S. C., Thornton, P. E., Bozbiyik, A., Fisher, R., Heald, C. L., Kluzek, E., Lamarque, J.-F., Lawrence, P. J., Leung, L. R., Lipscomb, W., Muszala, S., Ricciuto, D. M., Sacks, W., Sun, Y., Tang, J., and Yang, Z.-L.: Technical description of version 4.5 of the Community Land Model (CLM), NCAR Earth System Laboratory – Climate and Global Dynamics Division, Boulder, Colorado, Tech. Rep. TN-503+STR, 2013.

Parker, G. G., Harmon, M. E., Lefsky, M. A., Chen, J., van Pelt, R., Weiss, S. B., Thomas, S. C., Winner, W. E., Shaw, D. C., and Franklin, J. F.: Three-dimensional structure of an old-growth *Pseudotsuga-Tsuga* canopy and its implications for radiation balance, microclimate, and gas exchange, Ecosystems, 7, 440–453, 2004.

Parkinson, J. A.: Nitrogen and phosphorus retranslocation from needles of Douglas-fir growing on three site types, Master's thesis, University of British Columbia, Canada, 1983.

Prein, A. F., Holland, G. J., Rasmussen, R. M., Clark, M. P., and Tye, M. R.: Running dry: the U.S. Southwest's drift into a drier climate state, Geophys. Res. Lett., 43, 1272–1279, 2016.

Raczka, B., Duarte, H. F., Koven, C. D., Ricciuto, D., Thornton, P. E., Lin, J. C., and Bowling, D. R.: An observational constraint on stomatal function in forests: evaluating coupled carbon and water vapor exchange with carbon isotopes in the Community Land Model (CLM 4.5), Biogeosciences, 13, 5183–5204, 2016.

Reichstein, M., Falge, E., Baldocchi, D., Papale, D., Aubinet, M., Berbigier, P., Bernhofer, C., Buchmann, N., Gilmanov, T., Granier, A., Grnwald, T., Havrnkov, K., Ilvesniemi, H., Janous, D., Knohl, A., Laurila, T., Lohila, A., Loustau, D., Matteucci, G., Meyers, T., Miglietta, F., Ourcival, J.-M., Pumpanen, J., Rambal, S., Rotenberg, E., Sanz, M., Tenhunen, J., Seufert, G., Vaccari, F., Vesala, T., Yakir, D., and Valentini, R.: On the separation of net ecosystem exchange into assimilation and ecosystem respiration: review and improved algorithm, Global Change Biol., 11, 1424–1439, 2005.

Sellers, P. J., Randall, D. A., Collatz, G. J., Berry, J. A., Field, C. B., Dazlich, D. A., Zhang, C., Collelo, G. D., and Bounoua, L.: A revised land surface parameterization (SiB2) for atmospheric GCMs. Part I: model formulation, J. Climate, 9, 676–705, 1996.

Shaw, D. C., Franklin, J. F., Bible, K., Klopatek, J., Freeman, E., Greene, S., and Parker, G. G.: Ecological setting of the Wind River old-growth forest, Ecosystems, 7, 427–439, 2004.

Sheffield, J. and Wood, E. F.: Projected changes in drought occurrence under future global warming from multi-model, multi-scenario, IPCC AR4 simulations, Clim. Dynam., 31, 79–105, 2008.

Spies, T. A., Giesen, T. W., Swanson, F. J., Franklin, J. F., Lach, D., and Johnson, K. N.: Climate change adaptation strategies for federal forests of the Pacific Northwest, USA: ecological, policy, and socio-economic perspectives, Landscape Ecol., 25, 1185–1199, 2010.

Swain, S. and Hayhoe, K.: CMIP5 projected changes in spring and summer drought and wet conditions over North America, Clim. Dynam., 44, 2737–2750, 2015.

Taylor, A. J., Lai, C.-T., Hopkins, F. M., Wharton, S., Bible, K., Xu, X., Phillips, C., Bush, S., and Ehleringer, J. R.: Radiocarbon-based partitioning of soil respiration in an old-growth coniferous forest, Ecosystems, 18, 459–470, 2015.

Thornton, P. E. and Zimmermann, N. E.: An improved canopy integration scheme for a land surface model with prognostic canopy structure, J Climate, 20, 3902–3923, 2007.

Thornton, P., Law, B., Gholz, H. L., Clark, K. L., Falge, E., Ellsworth, D., Goldstein, A., Monson, R., Hollinger, D., Falk, M., Chen, J., and Sparks, J.: Modeling and measuring the effects of disturbance history and climate on carbon and water budgets in evergreen needleleaf forests, Agr. Forest Meteorol., 113, 185–222, 2002.

Unsworth, M. H., Phillips, N., Link, T., Bond, B. J., Falk, M., Harmon, M. E., Hinckley, T. M., Marks, D., and Paw U, K. T.: Components and controls of water flux in an old-growth Douglas-fir–western hemlock ecosystem, Ecosystems, 7, 468–481, 2004.

van Mantgem, P. J., Stephenson, N. L., Byrne, J. C., Daniels, L. D., Franklin, J. F., Fulé, P. Z., Harmon, M. E., Larson, A. J., Smith, J. M., Taylor, A. H., and Veblen, T. T.: Widespread increase of tree mortality rates in the western United States, Science, 323, 521–524, 2009.

Wharton, S., Falk, M., Bible, K., Schroeder, M., and Paw U, K.: Old-growth CO_2 flux measurements reveal high sensitivity to climate anomalies across seasonal, annual and decadal time scales, Agr. Forest Meteorol., 161, 1–14, 2012.

White, M. A., Thornton, P. E., Running, S. W., and Nemani, R. R.: Parameterization and sensitivity analysis of the BIOME-BGC terrestrial ecosystem model: net primary production controls, Earth Interact., 4(Paper no. 3), 1–80, 2000.

Williams, M., Woodward, F. I., Baldocchi, D. D., and Ellsworth, D.: CO_2 capture — leaf to landscape (Chapter 6), in: Photosynthetic adaptation: chloroplast to landscape, Ecological Studies, 178, Smith, W. K., Vogelmann, T. C., and Critchley, C. (Eds.), Springer Science and Business Media Inc., New York, USA, 133–170, 2004.

Woodruff, D. R., Bond, B. J., and Meinzer, F. C.: Does turgor limit growth in tall trees?, Plant Cell Environ., 27, 229–236, 2004.

Biogeosciences Discuss., doi:10.5194/bg-2016-441, 2016
Manuscript under review for journal Biogeosciences
Published: 21 October 2016

Table 1. Summary of changes in CLM parameters during the calibration process. The parameters listed, excluding M, Q_{10}, m_{bb}, b_{bb}, and soil hydraulic parameters, correspond to the needleleaf evergreen temperate tree plant functional type (NETT PFT).

Parameter	Description	CLM name	Default CLM value	Calibrated CLM value
$A_{s:l}$	New stem C: new leaf C ratio (gC gC^{-1})	*stem_leaf*	Dynamic	2
$A_{fr:l}$	New fine root C: new leaf C ratio (gC gC^{-1})	*froot_leaf*	1	0.385
CN_l	Leaf C:N ratio (gC gN^{-1})	*leafcn*	35	38.2
CN_{llit}	Leaf litter C:N ratio (gC gN^{-1})	*lflitcn*	70	76.4
CN_{fr}	Fine root C:N ratio (gC gN^{-1})	*frootcn*	42	64.7
τ_l	Leaf longevity (yr)	*leaf_long*	3	5
r_b	Root distribution parameter (m^{-1})	*rootb_par*	2	1
SLA_0	Specific leaf area at canopy top (m^2 leaf gC^{-1})	*slatop*	0.010	0.006
m	SLA(x) slope (m^2 ground gC^{-1})	*dsladlai*	0.00125	0.000985
M	Plant mortality rate (% yr^{-1})	*am*	2	1.5
Q_{10}	Temperature sensitivity coefficient of maintenance respiration and decomposition (–)	*q10*	1.5	2.5
Soil hydraulic parameters	Version used	*origflag* (namelist variable)	0 (CLM4.5)	1 (CLM4.0)
m_{bb}	Ball-Berry Eq. slope (–)	*mbbopt*	9	6
b_{bb}	Ball-Berry Eq. intercept (µmol m^{-2} leaf s^{-1})	*bbbopt*	10000	5000

Biogeosciences Discuss., doi:10.5194/bg-2016-441, 2016
Manuscript under review for journal Biogeosciences
Published: 21 October 2016

Table 2. Modeled leaf area index, biomass, and $\delta^{13}C$ values vs. observations. CLM results reported here are annual averages at the end of the transient run (year 2006). CLM $\delta^{13}C$ values were calculated from annual averages of the respective ^{13}C and ^{12}C pools.

Variable	CLM	Observation	Reference
LAI (m^2 leaf m^{-2} ground)	8.0	9.3 ± 2.1	AmeriFlux database
Leaf carbon (gC m^{-2} ground)	855	941 ± 322	AmeriFlux database
Fine root carbon (gC m^{-2} ground)	329	362 ± 26	AmeriFlux database
Tree wood carbon (gC m^{-2} ground)	22946	21918 ± 1349	AmeriFlux database
Coarse root carbon (gC m^{-2} ground)	6884	8122 ± 639	AmeriFlux database
SOM carbon, 0–1 m (gC m^{-2} ground)	24689		
$\delta^{13}C$ leaf (‰)	−28.401	−28.2 to −26.3 (TC[a])	Fessenden and Ehleringer (2003), Fig. 2b
		−29.5 to −28.2 (MC[a])	
		−34.2 to −32.4 (BC[a])	
$\delta^{13}C$ SOM, 0–1 m (‰)	−26.294	−26.5 to −25.0 (20 cm)	Fessenden and Ehleringer (2003), Fig. 3

[a] TC, MC, and BC stands for top, middle, and bottom canopy, respectively

Biogeosciences Discuss., doi:10.5194/bg-2016-441, 2016
Manuscript under review for journal Biogeosciences
Published: 21 October 2016

Figure 1. Location and view of the Wind River AmeriFlux site, US-Wrc (satellite image from Google Earth).

Biogeosciences Discuss., doi:10.5194/bg-2016-441, 2016
Manuscript under review for journal Biogeosciences
Published: 21 October 2016

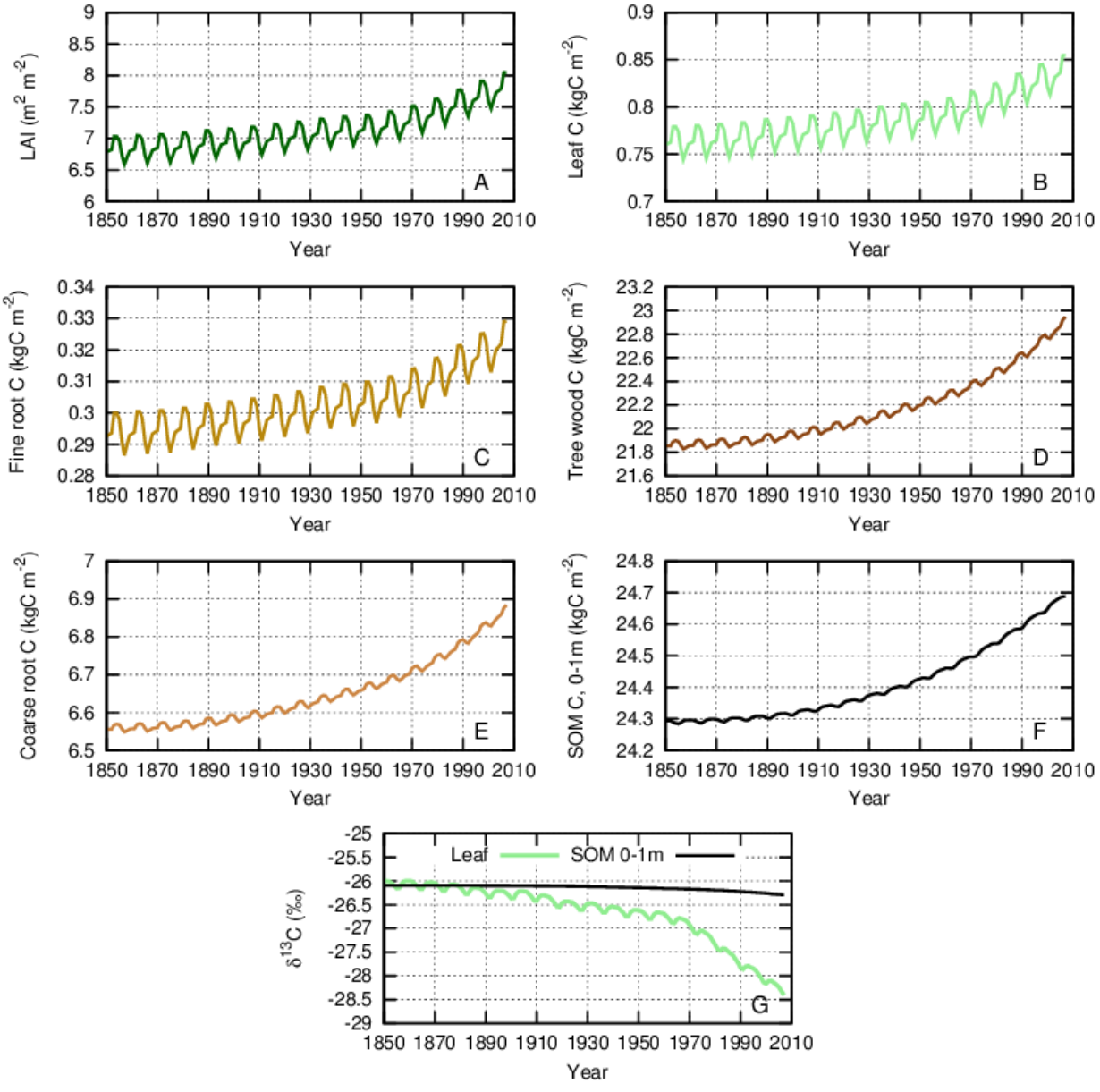

Figure 2. Modeled leaf area index (A), carbon stocks (B–F), and $\delta^{13}C$ of leaf and soil organic matter (G) during the transient run. Values in panels A–F correspond to annual averages. The $\delta^{13}C$ values in panel G were calculated from annual averages of the respective ^{13}C and ^{12}C pools.

Biogeosciences Discuss., doi:10.5194/bg-2016-441, 2016
Manuscript under review for journal Biogeosciences
Published: 21 October 2016

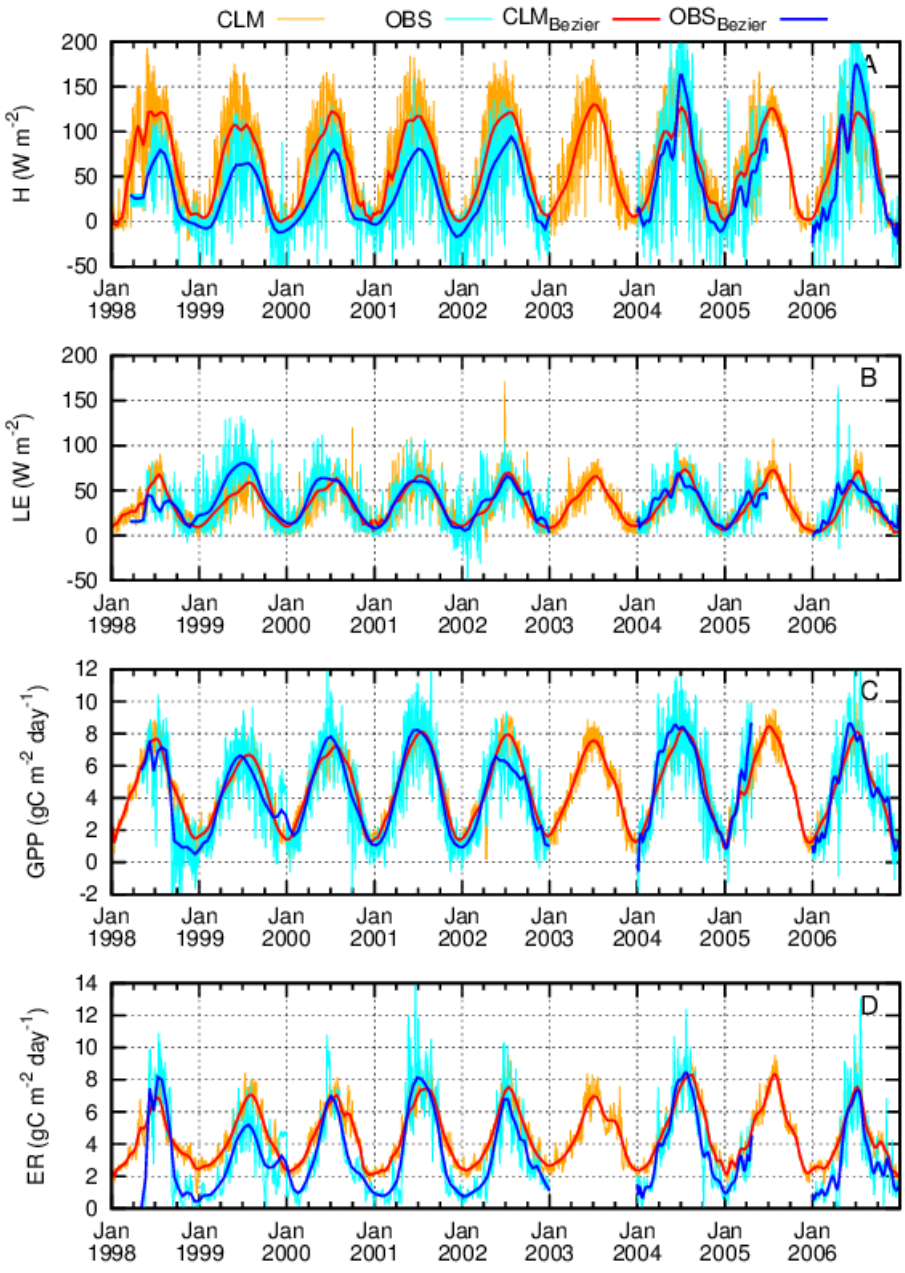

Figure 3. Modeled sensible heat flux (A), latent heat flux (B), gross primary production (C), and ecosystem respiration (D) vs. site observations. Orange/red and cyan/blue lines correspond to modeled and observed values, respectively. For a clearer visualization, the daily averages (thin lines) were smoothed with a Bézier algorithm (thick lines).

Biogeosciences Discuss., doi:10.5194/bg-2016-441, 2016
Manuscript under review for journal Biogeosciences
Published: 21 October 2016

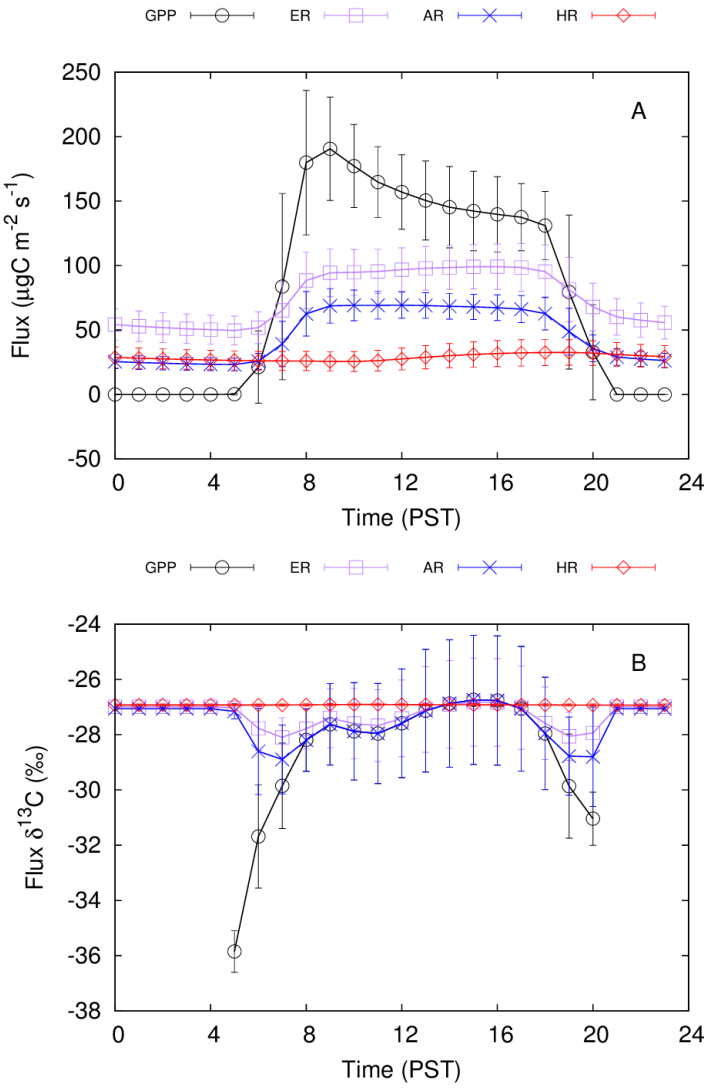

Figure 4. Mean diurnal cycle of modeled carbon fluxes (A) and their respective carbon isotope ratios (B) for the summer months (June–September) of years 1998–2006. Fluxes include gross primary production (black circles), ecosystem respiration (purple squares), autotrophic respiration (blue crosses), and heterotrophic respiration (red diamonds). Bars correspond to ±1 standard deviation.

Biogeosciences Discuss., doi:10.5194/bg-2016-441, 2016
Manuscript under review for journal Biogeosciences
Published: 21 October 2016

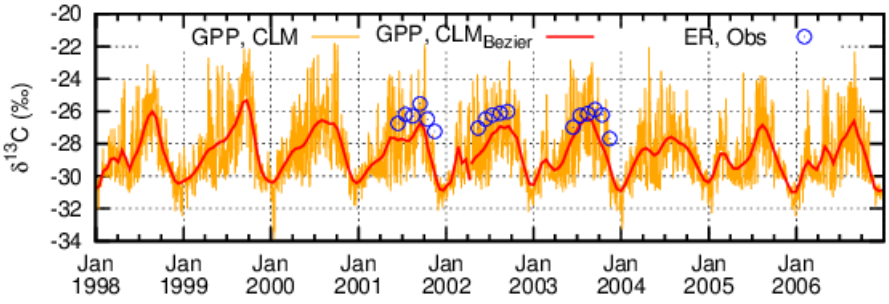

Figure 5. Modeled $\delta^{13}C$ of gross primary production (lines) and observed $\delta^{13}C$ of ecosystem respiration (circles). Thin orange line corresponds to daily averages using 10:00–16:00 data only. For a clearer visualization, this curve was smoothed with a Bézier algorithm (thick red line). Blue circles correspond to site observations (monthly averages) reported by Lai et al. (2005).

Biogeosciences Discuss., doi:10.5194/bg-2016-441, 2016
Manuscript under review for journal Biogeosciences
Published: 21 October 2016

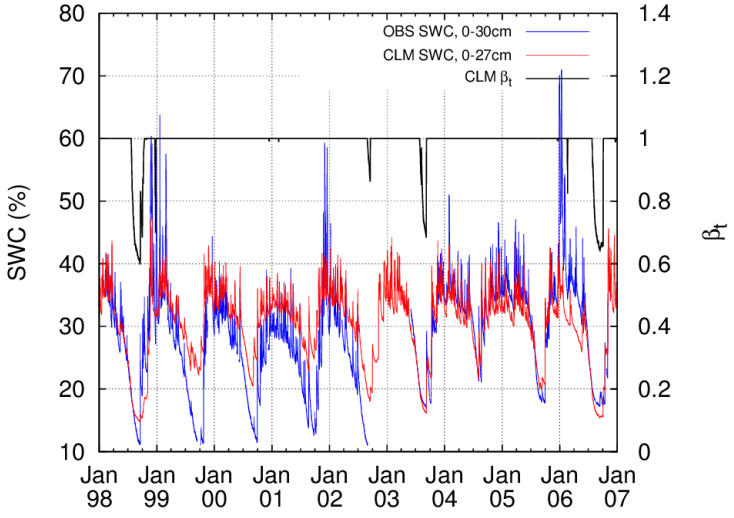

Figure 6. Hourly soil water content and CLM's drought stress parameter, β_t (black line). Observed SWC (blue line) corresponds to the integrated value for the top 30 cm of soil, while modeled SWC (red line) corresponds to the integrated value for the top 5 soil layers in CLM (0–27 cm).

Biogeosciences Discuss., doi:10.5194/bg-2016-441, 2016
Manuscript under review for journal Biogeosciences
Published: 21 October 2016

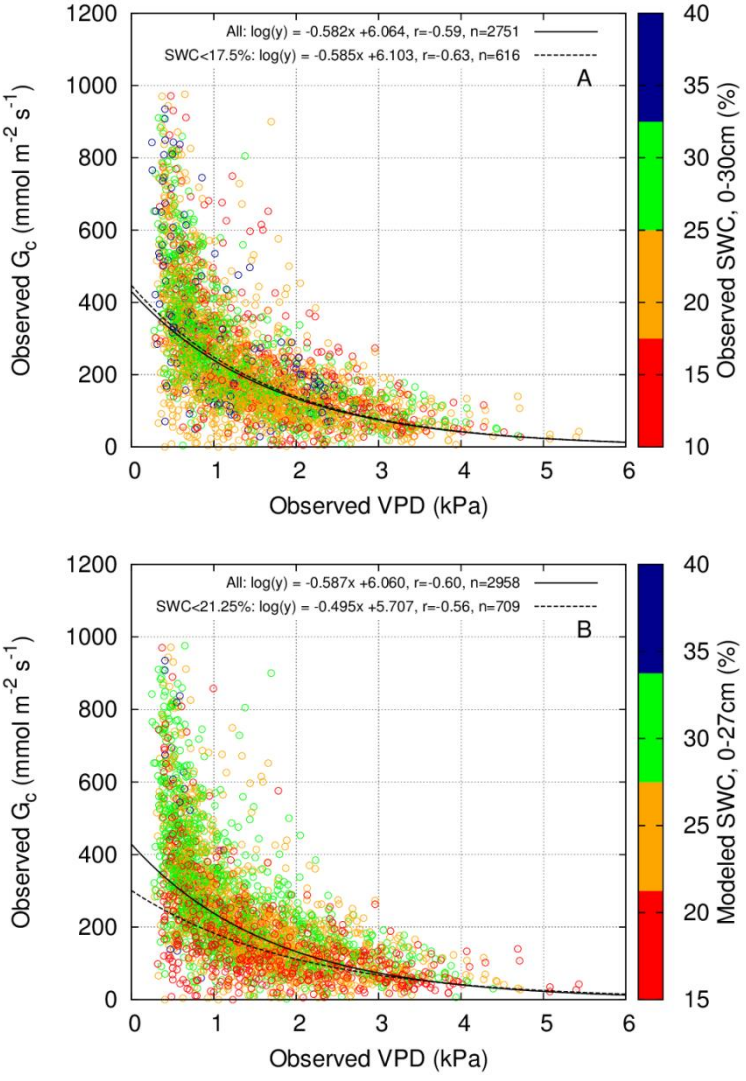

Figure 7. Hourly observed canopy conductance vs. observed VPD for the summer months (June–September) of years 1999–2006, restricted to 10:00–16:00 PST (additional restrictions were imposed to the calculation of G_c, see Sect. 2.7). Years 1998 and 2005 were not included due to missing data. Data points were segregated according to observed SWC in panel A and according to modeled SWC in panel B (see Fig. 6). Lines correspond to the linear regression between $\log G_c$ and VPD using all data points (solid lines) and using only points within the lowest SWC bin (red circles, dashed lines).

Biogeosciences Discuss., doi:10.5194/bg-2016-441, 2016
Manuscript under review for journal Biogeosciences
Published: 21 October 2016

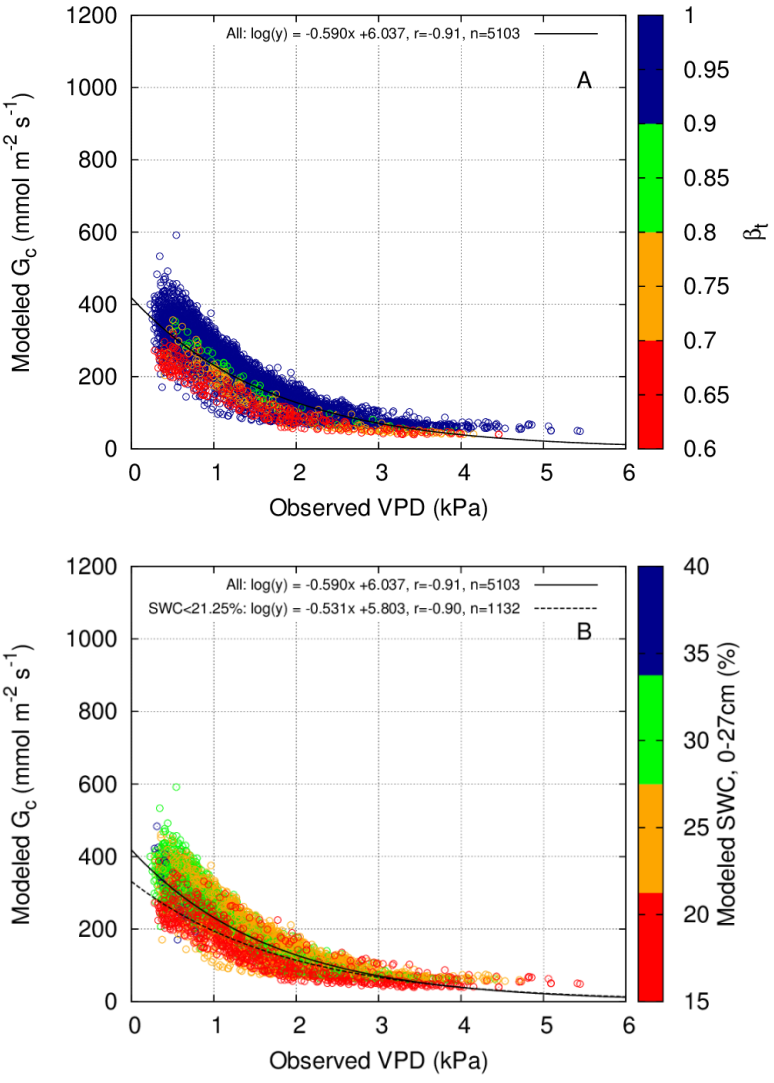

Figure 8. Hourly modeled canopy conductance vs. observed VPD for the summer months (June–September) of years 1999–2006, restricted to 10:00–16:00 PST (additional restrictions were imposed to the calculation of G_c, see Sect. 2.7). Note that observed air temperature and relative humidity were used to drive CLM. Years 1998 and 2005 were not included for consistency with Fig. 7. Data points were segregated according to the drought stress parameter β_t in panel A and according to modeled SWC in panel B (see Fig. 6). Lines correspond to the linear regression between $\log G_c$ and VPD using all data points (solid lines) and using only points within the lowest SWC bin (red circles, dashed line).

Biogeosciences Discuss., doi:10.5194/bg-2016-441, 2016
Manuscript under review for journal Biogeosciences
Published: 21 October 2016

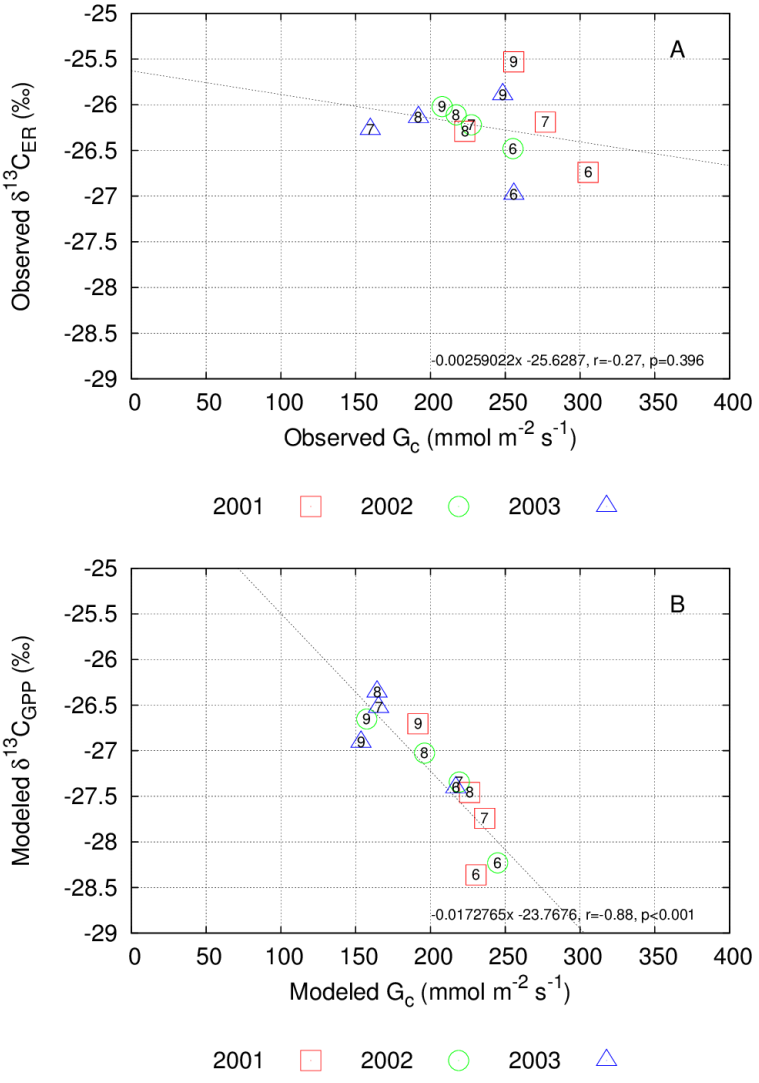

Figure 9. Observed $\delta^{13}C$ of ecosystem respiration vs. observed canopy conductance (A) and modeled $\delta^{13}C$ of gross primary production vs. modeled canopy conductance (B) for the summer months of 2001–2003. Except for the observed $\delta^{13}C_{ER}$, data points correspond to monthly averages of daytime (10:00–16:00) data (additional restrictions were imposed to the calculation of G_c, see Sect. 2.7). Observed $\delta^{13}C_{ER}$ corresponds to the monthly averages reported by Lai et al. (2005). Numbers at the center of each point indicate the month.

Biogeosciences Discuss., doi:10.5194/bg-2016-441, 2016
Manuscript under review for journal Biogeosciences
Published: 21 October 2016

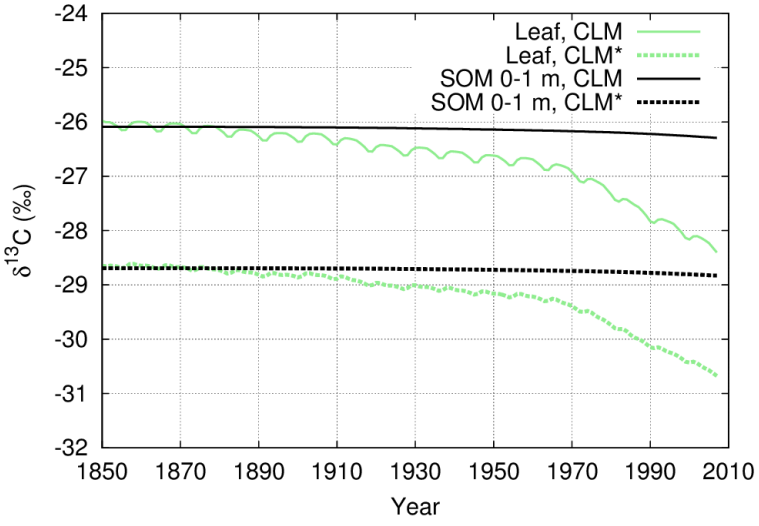

Figure A1. Modeled $\delta^{13}C$ of leaf and soil organic matter (calculated from annual averages of the respective ^{13}C and ^{12}C pools) during the transient run (green and black lines, respectively). Results from two model configurations are presented: CLM (calibrated model, solid lines) and CLM* (calibrated model using the default stomatal conductance parameters (m_{bb} and b_{bb}; see Table 1), dashed lines). cf. Table 2.

Biogeosciences Discuss., doi:10.5194/bg-2016-441, 2016
Manuscript under review for journal Biogeosciences
Published: 21 October 2016

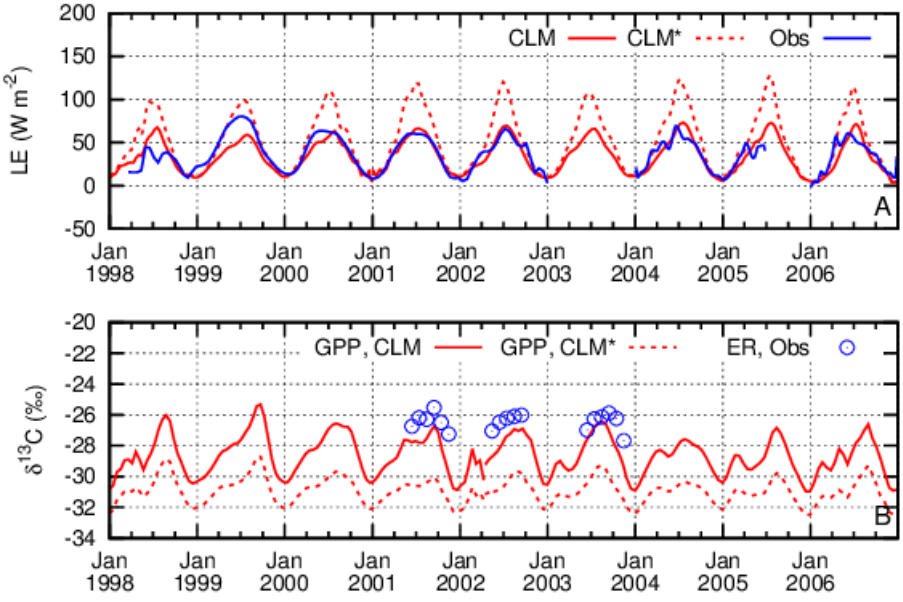

Figure A2. Modeled latent heat flux (A) and $\delta^{13}C$ of gross primary production (B, lines) for 1998–2006. The curves presented correspond to Bézier-smoothed daily averages as in Figs. 3 and 5. Results from two model runs are presented: CLM (calibrated model, solid red lines), and CLM* (calibrated model using the default stomatal conductance parameters (m_{bb} and b_{bb}; see Table 1), dashed red lines). The blue line and circles correspond to site observations. The circles in panel B are the monthly averages of $\delta^{13}C_{ER}$ reported by Lai et al. (2005).